Current Research (2016) Newfoundland and Labrador Department of Natural Resources
Geological Survey, Report 16-1, pages 39-69

PRELIMINARY U–Pb GEOCHRONOLOGY AND PETROCHEMISTRY OF VOLCANIC ROCKS AND FELSIC DYKES OF THE SILURIAN SOPS ARM GROUP, WHITE BAY, WESTERN NEWFOUNDLAND (NTS 12H/10 and 15)

H.A.I. Sandeman and G.R. Dunning[1]
Mineral Deposits Section
[1]Department of Earth Sciences, Memorial University of Newfoundland,
St. John's, NL, A1B 3X5

ABSTRACT

The Sops Arm group is a sequence of subaerial volcanic rocks, terrestrial sedimentary rocks, and shallow-marine sedimentary rocks that define a Silurian volcano-sedimentary basin in western White Bay (NTS map areas 12H/10 and 15). The Sops Arm group is divided into a Western sequence, including the volcanic Pollards Point formation and terrestrial to fluvial sedimentary rocks of the Jackson's Arm and Frenchmans Cove formations, and an Eastern sequence, including the shallow-marine rocks of the Simms Ridge and Natlins Cove formations. The latter include mafic and felsic volcanic rocks, termed the Sops Island volcanic member. The Western and Eastern sequences are separated by an arcuate, moderately east-dipping high-strain zone termed the Long Steady fault: a structure that likely has a complex history, possibly including thrust motions.

The Western and Eastern sequences are both characterized by intercalated mafic and felsic lava flows, felsic welded tuff and volcanic breccia, agglomerate and volcanogenic conglomerate, sandstone and siltstone. Mafic volcanic rocks of both sequences are chemically similar, transitional to calc-alkaline continental basalts derived from a weakly enriched mantle source. Felsic volcanic rocks consist of a wide range of alkaline, within-plate (A-type) rhyolitic, upper crustal fractionates, whereas felsic dykes appear to represent partial melts of hornblende and/or garnet-bearing lower crust.

The only constraint on the age of the Sops Arm group is based on poorly documented Telychian to Pridoli macrofossil assemblages in the sandstones of the Eastern sequence. New U–Pb zircon geochronology indicates that rhyolite near the structural base of the Western sequence formed at 434.3 ± 1.1 Ma, which is the oldest age documented for a Silurian cover sequence in the Newfoundland Appalachians. A syn- to posttectonic felsic dyke that cuts the lower Simms Ridge Formation of the Eastern sequence yielded a crystallization age of 401.1 ± 0.8 Ma, indicating Devonian magmatic activity. The ^{40}Ar–^{39}Ar step-heating analysis of muscovite from foliated, muscovite–quartz–albite–ankerite-schist cut by a massive quartz–ankerite–pyrite–chalcopyrite–galena vein at the Browning Mine (adjacent to the Long Steady fault) yielded a plateau age of 374 ± 1 Ma, constraining the timing of precious-metal mineralization to the Frasnian.

INTRODUCTION

The Sops Arm group of western White Bay (NTS map areas 12H/10 and 15) is the only Silurian volcano-sedimentary cover sequence in the Humber Zone, and the most northwesterly sequence of its type in the Newfoundland Appalachians (Figure 1). The Sops Arm group, as well as surrounding rocks of the western White Bay area, have a rich history of exploration and mining that started with the discovery of gold at Pollards Point and the opening of the Browning Mine (Martin, 1983; Kerr, 2006a). The discovery of gold at the Browning Mine rapidly led to the recognition of a number of other gold-mineralized zones in the Sops Arm group, such as the Unknown Brook, Simms Ridge, West Corner Brook and Freemans prospects (*see* Kerr, 2006a; Figure 2). Much of the exploration history of the region up to 2006, and the development of ideas about regional geology and stratigraphy, are detailed in Kerr (2003, 2004, 2006a, b). Kerr and Knight (2004) and Kerr (2006a) outline the uncertainties and issues associated with our present state of knowledge of the geological evolution of the region. The most critical gap is a dearth of modern U–Pb geochronological and lithogeochemical data for the volcanic, plutonic and meta-igneous rocks of the region and, in particular, for the rocks of the Sops Arm group.

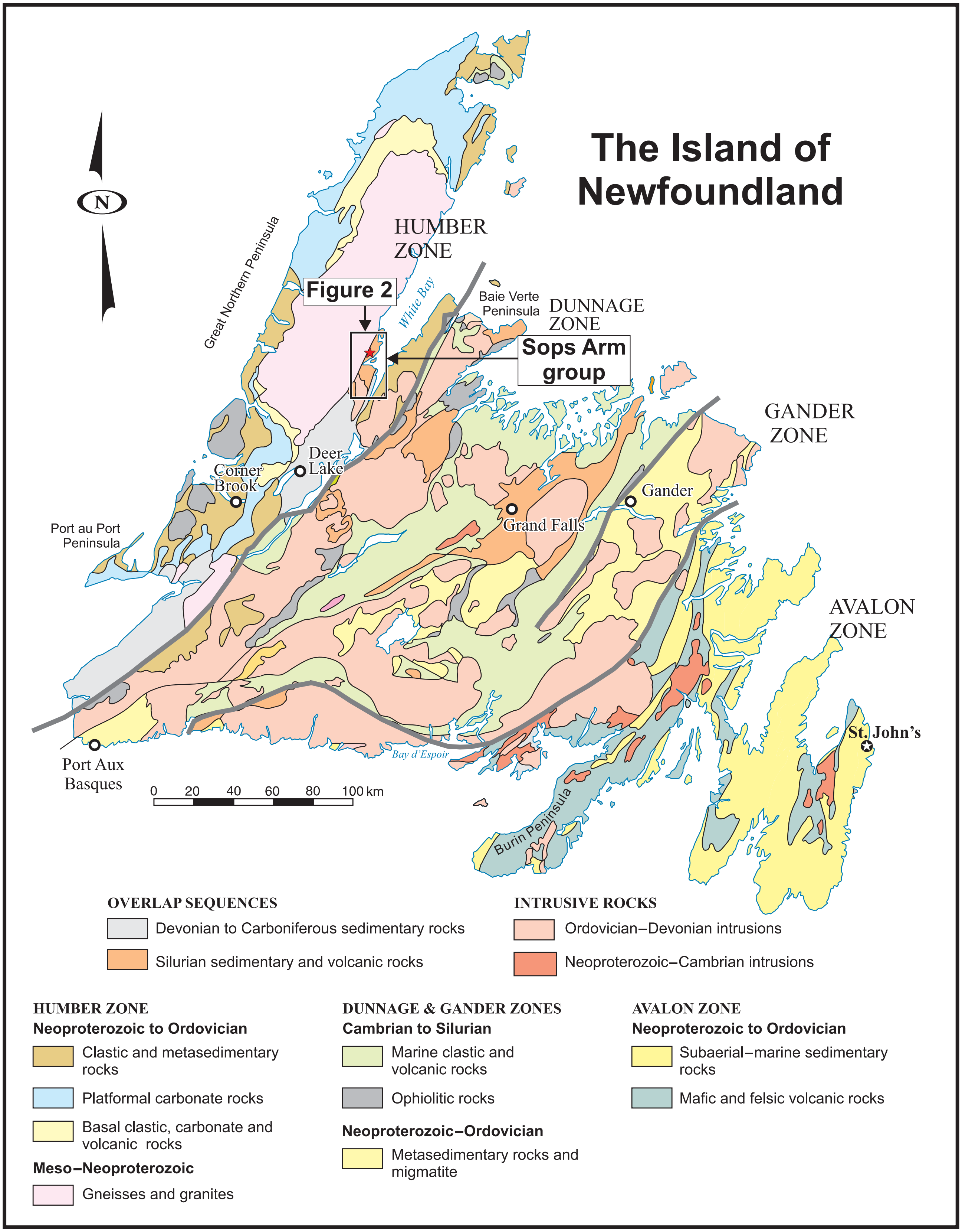

Figure 1. *Simplified geological map of Newfoundland showing the location of the Sops Arm group with respect to major geological terranes and tectonic boundaries (after Colman-Sadd* et al.*, 1990).*

Since 2006, renewed mineral exploration in the region has led to the discovery of a number of new gold-mineralized areas, including the Thor and Kramer quartz vein systems in the Precambrian basement to the west of the Doucers Valley Fault (Figure 2; Ebert, 2008, 2009, 2010; Froude, 2011a, b) and the Shrik, Boot n Hammer and Stocker zones, occurring in the Sops Arm group and Coney Head complex west-northwest of Frenchman's Cove (Figure 2; *http://www.metalscreek.com/article/Jackson's-arm—nfld-267.asp*). Work by mineral exploration companies (*e.g.*, Churchill and Voordouw, 2006; Ebert, 2008, 2009, 2010; Fitzpatrick and Osmond, 2010; Froude, 2011a, b; Harris, 2008; McLennon, 2010; Murphy and Smith, 2007; O'Driscoll, *et al.*, 2011; Patey, 2010; Patey and King, 2010; Reid, 2009; Reid *et al.*, 2008; Thurlow *et al.*, 2007), along with governmental and academic studies (Kerr and van Breemen, 2007; Minnett, 2012; Minnett *et al.*, 2010, 2012), have also generated new information about the mineralization in the Sops Arm group and the geology of the wider White Bay area.

Presently, the Sops Arm group is inferred to be Middle to Late Silurian, based on macrofossil assemblages in calcareous siltstone of the Simms Ridge and Natlins Cove formations; these rocks belong to the Telychian and Pridoli stages. This contribution reports new field and petrographic observations, as well as chemical abrasion (CA)-TIMS U–Pb zircon geochronology for two felsic igneous rocks in the area. It also discusses a preliminary lithogeochemical dataset for twenty-nine samples of mafic and felsic volcanic rocks and six felsic dykes that cut the rocks of the Sops Arm group. An ^{40}Ar–^{39}Ar step-heating age for fabric-forming muscovite from a schistose siltstone hosting the postorogenic gold-bearing veins at the Browning Mine provides constraints on the timing of mineralization. These new data are evaluated and discussed and potential avenues for future research are outlined.

REGIONAL SETTING

Western White Bay (Figures 1 and 2) is transected by three major north–south-trending, typically steeply dipping faults, termed the Cabot, the Birchy Ridge and the Doucers Valley faults (Smyth and Schillereff, 1982). The Sops Arm group lies between the latter two faults, separated from the Carboniferous Anguille Group to the east by the Birchy Ridge Fault and the Precambrian and Cambro-Ordovician rocks of the Long Range Inlier to the west by the Doucers Valley Fault (Figure 2). The Doucers Valley Fault comprises a number of broadly parallel, steeply dipping, crustal-scale faults forming a ~500-m-wide-zone that exhibits a long and episodic history of displacement (*e.g.*, Lock, 1969a; Smyth and Schillereff, 1982; Tuach, 1987). It separates the Ordovician intra-oceanic ophiolitic rocks of the Southern White Bay allochthon and unconformably overlying Silurian continental cover sequences in the east, from the Precambrian (Grenvillian) basement of the Long Range Inlier and autochthonous Cambrian to Ordovician platformal cover rocks in the west (Kerr and Knight, 2004). The Long Range Inlier (Erdmer, 1986; Kamo *et al.*, 1989; Kamo and Gower, 1994; Hinchey, 2010) is unconformably overlain by a narrow belt of Cambro-Ordovician platformal shelf rocks of the Labrador, Port-au-Port, St. George and Table Head groups, which is structurally overlain to the east by the disrupted, Southern White Bay Allochthon (Smyth and Schillereff, 1982; Kerr and Knight, 2004; Figure 2). The latter includes assorted clastic sedimentary rocks, metavolcanic rocks, minor ultramafic rocks as well as trondhjemite/tonalite and monzogranite (Coney Head complex; Williams, 1977). The Coney Head complex is exposed on Coney Head, immediately north of Frenchman's Cove (Figure 2).

Along its western margin, the Sops Arm group is in fault contact with the Cambro-Ordovician rocks of the Southern White Bay Allochthon or the Cambro-Ordovician platformal rocks (Smyth and Schillereff, 1982; Kerr and Knight, 2004; Figure 2). At its northern extremity near Frenchman's Cove (Figure 2), matrix-supported pebble- and boulder-conglomerate and mafic and felsic volcanic units of the Sops Arm group unconformably overlie variably silica–sericite–goethite-altered trondhjemite–tonalite of the Coney Head complex (Williams, 1977; Smyth and Schillereff, 1982; Dunning, 1987; Kerr, 2006a; *this study*). Clasts in the conglomerates include tonalite, similar to that of the Coney Head complex. The unconformity is difficult to trace, and is strongly disrupted by subsequent folding and faulting. The underlying tonalite–trondhjemite, the conglomerates and the mafic and felsic volcanic units are all interleaved on a scale of 10s to 100s of metres, indicating late imbrication of the group and its substrate.

Tonalite of the Coney Head complex yielded a relatively simple concordant U–Pb zircon age of 474 ± 2 Ma indicating that it crystallized in the Ordovician (Floian stage), prior to tectonic emplacement onto the Laurentian margin (Dunning, 1987). The Coney Head complex is interpreted as the plutonic infrastructure of an Ordovician island arc that formed in Iapetus and was tectonically emplaced onto the Laurentian margin accompanying *ca.* 470 Ma Taconic orogenesis (Williams, 1977; van Staal *et al.*, 2009). A second U–Pb age on titanite and zircon from graphic-textured biotite-microgranite that crosscuts this tonalite yielded a more complex, lower concordia intercept age of 432 ± 2 Ma (Dunning, 1987). This Silurian (Sheinwoodian) age indicates that the microgranite stitched the Coney Head complex to the Laurentian basement (Dunning, *op. cit.*) and may

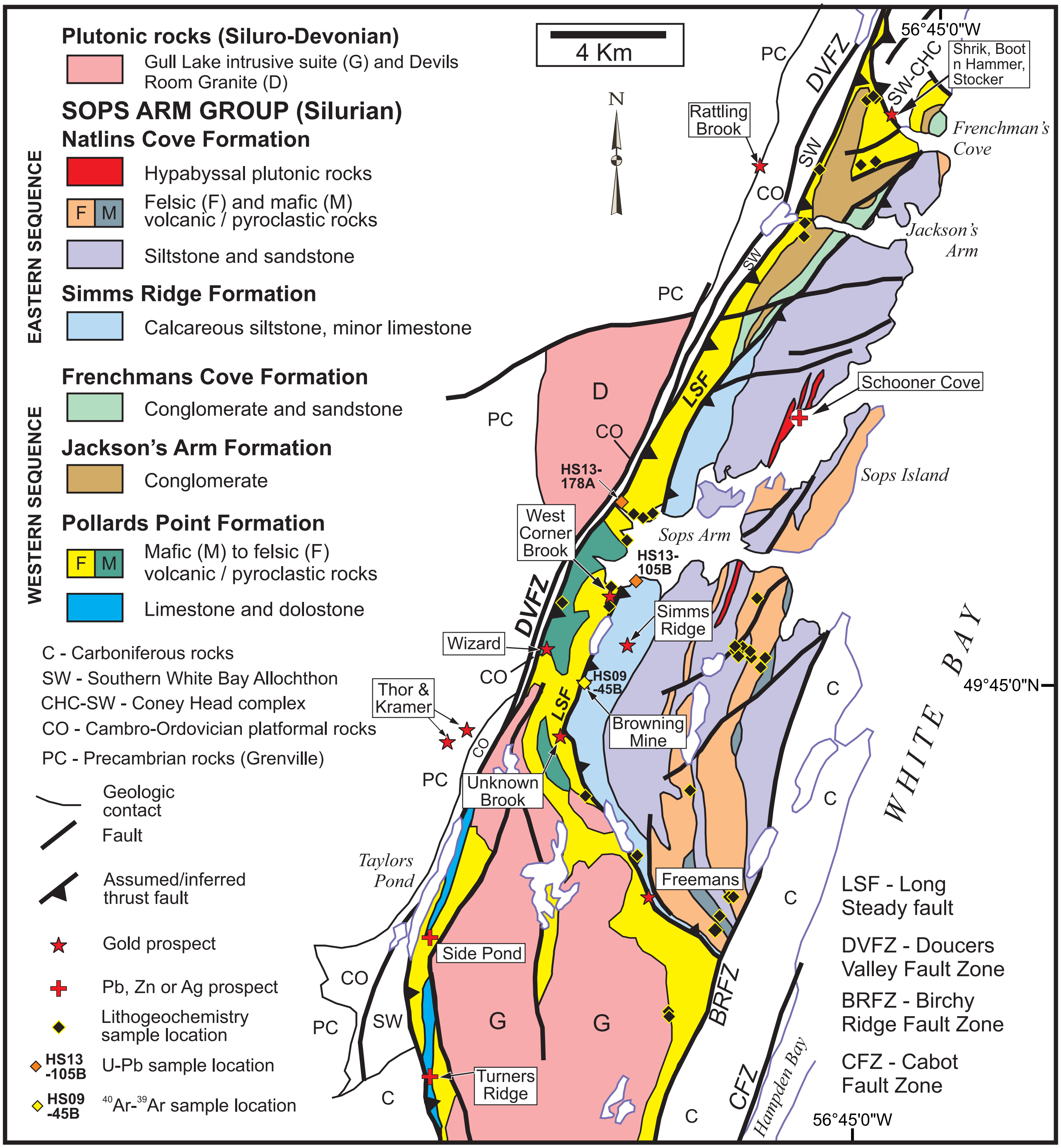

Figure 2. *Simplified geology of the western White Bay area and the Sops Arm group (modified after Kerr, 2006a). Approximate locations of the U–Pb zircon samples, the ^{40}Ar–^{39}Ar muscovite sample as well as the distribution of lithogeochemistry sample sites are indicated. Also shown are the locations of precious- and base-metal showings (Kerr, 2006b).*

be related to the Sops Arm group felsic volcanic rocks. The age of the Sops Arm group is not constrained by geochronology, but only on the basis of poorly documented Silurian (Telychian to Pridoli; *ca.* 438–419 Ma) macrofossil assemblages from the Natlins Cove Formation of the Eastern sequence (Heyl, 1937; Shrock and Twenhofel, 1939; Lock, 1969a, b; Berry and Boucot, 1970; Boyce *et al.*, 1993). A better understanding of the fossil assemblages in the Natlins

Cove Formation and other units of the Sops Arm group would greatly advance our understanding of the chronostratigraphy of these Silurian rocks.

OVERVIEW OF THE GEOLOGY OF THE SOPS ARM GROUP

The geology of the Sops Arm group and its constituent formations has been extensively described by Heyl (1937), Betz (1948), Lock (1969a, b), Smyth and Schillereff (1982) and Kerr (2006a). The last two contributions proposed a two-fold subdivision of the group into Western and Eastern sequences, dissected by an east-dipping (~30°) high-strain zone termed the Long Steady fault (Kerr, 2006a; Figures 2 and 3). This two-sequence interpretation is used as the basis for a chemostratigraphic subdivision of the group. The individual constituent formations are described in previous contributions (Heyl, 1937; Betz, 1948; Neale and Nash, 1963; Lock, 1969a; Smyth and Schillereff, 1982; Kerr, 2006a), and the following account emphasizes new salient field observations and clarifies some earlier discussions.

Volcanic and sedimentary rocks of the Western sequence are typically more highly strained than those in the east, in particular along its western boundary, in proximity to the Doucers Valley Fault (Figure 2). Other than compositional layering, primary textures are commonly overprinted and obscured, such that mafic volcanic rocks are preserved as chlorite schist and felsic rocks are represented by quartz–albite–sericite schist. The Eastern sequence is dominated by thicker, openly folded and less deformed, better preserved sequences of calcareous siltstone (locally fossiliferous) and sandstone. These occur in two discrete belts that are separated by a thick package of felsic and mafic flows and related volcanogenic sedimentary rocks. Previous reports have suggested that the Eastern sequence is largely homoclinal, upright, east-dipping and unaffected by structural repetition. Such a conclusion may, however, be premature and the structural interpretation of the Sops Arm group requires more detailed field study and structural analyses.

THE WESTERN SEQUENCE

POLLARDS POINT FORMATION

Following the suggestion of Kerr (2006a), the name Pollards Point formation (Figure 3) is used to replace the 'lower volcanic formation' of Smyth and Schillereff (1982) and the three formations proposed by Lock (1969a). The Pollards Point formation is best exposed around the western parts of Sops Arm and also north of Jackson's Arm (Figure 2). It includes felsic volcanic and pyroclastic rocks although

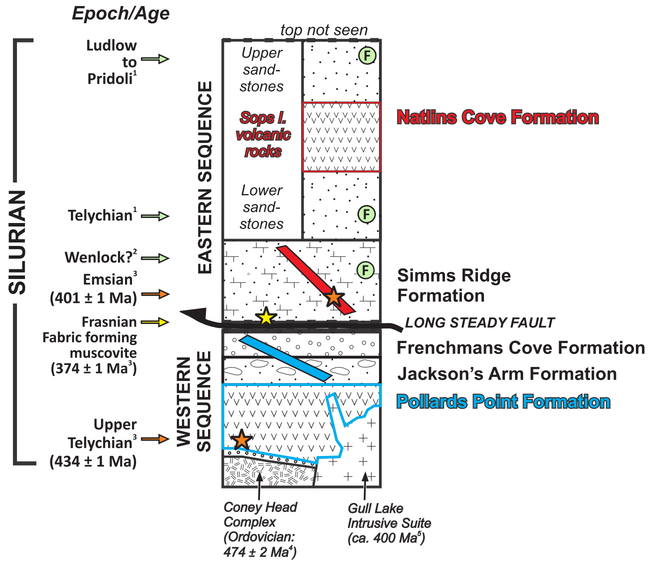

Figure 3. *Simplified lithostratigraphic column for units of the Sops Arm group (modified after Kerr, 2006a). Approximate stratigraphic locations of the U–Pb zircon and ^{40}Ar–^{39}Ar muscovite samples are indicated. Also shown are the approximate locations of macroscopic fossil localities and their implied biostratigraphic age constraints (International Chronostratigraphic Chart 2015/01: www.stratigraphy.org). Subscripts refer to data source: 1) Berry and Boucot (1970); 2) Lock (1969a); 3)* This study*; 4) Dunning (1987); 5) Erdmer (1986).*

mafic volcanic rocks are more common than previously reported and intermediate volcanic rocks are rare or absent. In the north, the formation is dominated by conglomerate and sandstone and subordinate volcanic rocks. The lowermost parts of the Pollards Point formation comprise either strongly sheared, sericitic felsic rocks in fault contact with older units (*e.g.*, immediately west of sample HS13-178A; Figure 2), or the cobble- to pebble-conglomerate that unconformably overlies tonalite of the Coney Head complex in the north near Frenchman's Cove (Figure 2). As previously mentioned, the unconformity is not easily recognized because of structural modification.

These lowermost units are overlain by a package of intercalated, dominantly felsic breccia (Plate 1A), flow-banded domes, tuffs and discontinuous, proximally derived, boulder to cobble conglomerate fans (*see* Plate 2 of Kerr 2006a). Epidote- and quartz-amygdaloidal mafic volcanic rocks are common (Plate 1B) and locally dominate the stratigraphy in the south (*e.g.*, south of Sops Arm; Figure 2) where pillows have been noted. Kerr (2006a) states, "the Pollards Point formation is varied and complex, and undoubtedly has marked lateral facies variations." This statement is correct, in that the Jackson's Arm and Frenchmans Cove formations, defined in the north of the map area

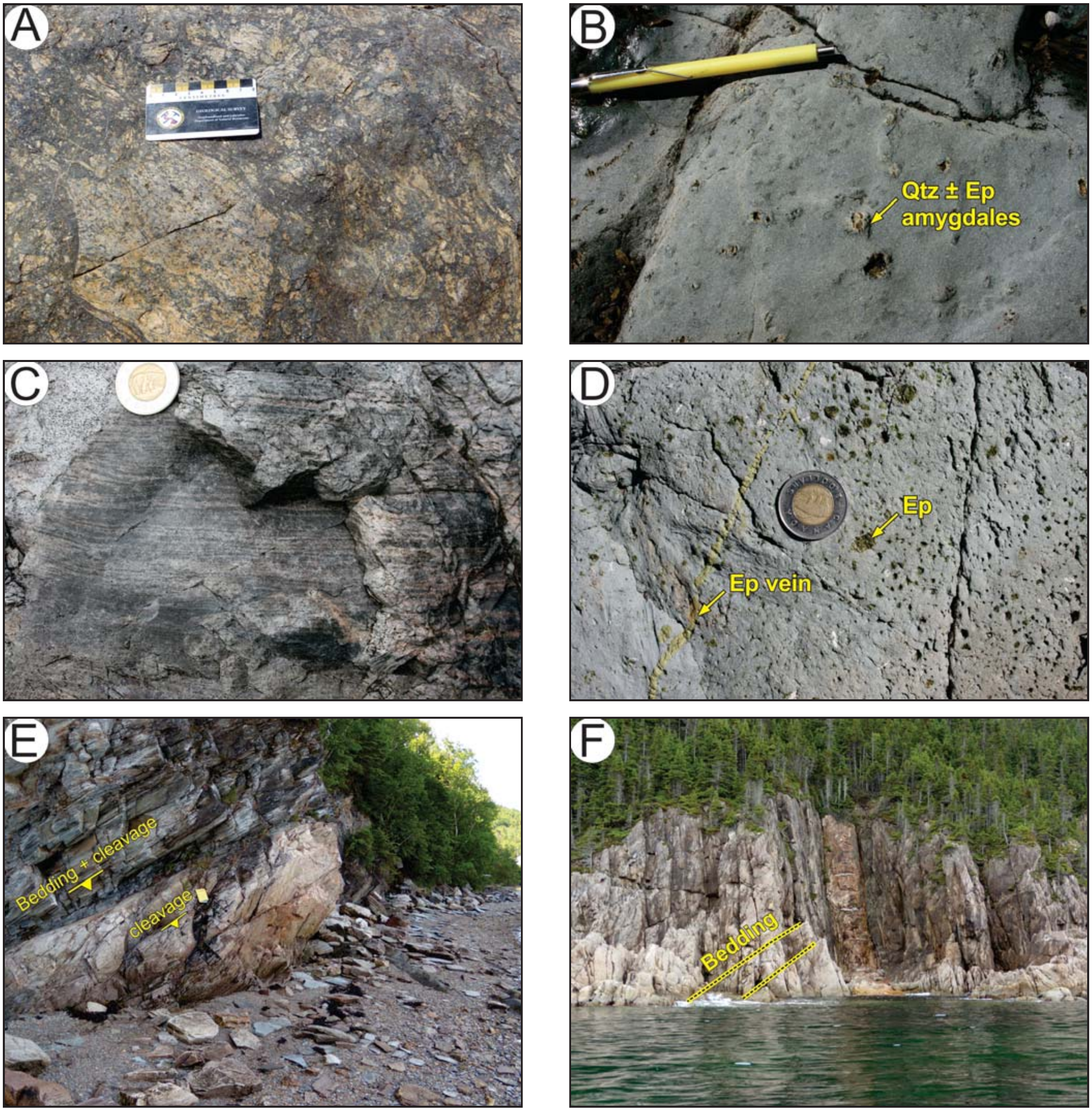

Plate 1. *Photos of representative rock types selected for lithogeochemistry. A) Autobrecciated, flow-banded rhyolite of the Pollards Point formation (location HS12-108). B) Variably schistose, epidote and quartz amygdaloidal basalt of the Pollards Point formation (sample HS13-140). Pen magnet is 12 cm in length. C) Flow-banded rhyolite of the volcanic rocks of the Natlins Cove Formation (HS10-70A). Two dollar coin for scale. D) Photograph of epidote amygdaloidal basalt of the Natlins Cove Formation (HS10-77). Two dollar coin is 2.8 cm in diameter. E) A 2-m-thick rhyolite dyke cuts schistose siltstone and sandstone of the Simms Ridge Formation (HS13-105B). The yellow notebook is 18 cm in height. F) A 4-m-wide rhyolite dyke cuts bedding in pebbly sandstone of the Frenchmans Cove formation (HS13-185).*

(Lock, 1969a; Smyth and Schillereff, 1982; Kerr, 2006a), are facies-equivalents of similar conglomerates preserved in the Pollards Point formation. Thus, the earlier view of the entire lower Sops Arm group as a single formation (*i.e.*, Giles Cove formation and subsidiary members), as suggested by Heyl (1937) and Betz (1948), may be more geologically accurate. South of Pollards Point, the formation appears to thin, is extensively intruded by younger plutonic rocks, and at its southern end is truncated by the Birchy Ridge fault.

JACKSON'S ARM FORMATION

This formation (Figures 2 and 3) is best exposed on the shores of Frenchman's Cove and in and around Jackson's Arm and consists of poorly sorted, polymict cobble- to boulder-conglomerate. The formation is not recognized in the south of the belt, but it is lithologically similar to thinner, discontinuous conglomerate units that are intercalated with basaltic and felsic volcanic rocks of the Pollards Point formation. The Jackson's Arm Formation conglomerates range from undeformed to foliated examples that have a well-developed, down-dip stretching lineation defined by elongated clasts (*see* Plates 3B, 3D, 10A, 10B in Kerr 2006a). Primary sedimentary features such as grading, cobble imbrication and crossbedding in sandy beds are present in the less deformed rocks. Mafic and felsic volcanic rocks (flows or tuff?) are also more common in the Jackson's Arm Formation than previously reported (*cf.* Smyth and Schillereff, 1982; Kerr, 2006a), notably, around Frenchman's Cove. The conglomerates are immature, coarse-grained volcanogenic rocks that likely formed as proximal debris, shed from felsic volcanic centres, and they have been interpreted to represent alluvial fan and fluvial deposits (Lock, 1969a, b).

FRENCHMANS COVE FORMATION

The Frenchmans Cove formation (Figures 2 and 3), introduced by Lock (1969a), conformably overlies the Jackson's Arm Formation and, although broadly similar, it is typically finer grained and better sorted (Lock, 1969a; Smyth and Schillereff, 1982; Kerr, 2006a). The formation is reported as unfossiliferous and is largely fluvial in origin. At its type locality, the Frenchmans Cove formation also includes mafic volcanic rocks and, to the north of Jackson's Arm, the structurally higher (eastern) parts exhibit moderate to strong deformation adjacent to the trace of the Long Steady fault. Inland exposures of the Frenchmans Cove formation between Jackson's Arm and Sops Arm are difficult to distinguish from the Jackson's Arm Formation. The Frenchmans Cove formation has been described to thin toward the south and disappears southward from Jackson's Arm. It was suggested that both have been excised by the Long Steady fault (*see* Smyth and Schillereff, 1982; Kerr, 2006a; Figures 2 and 3), but facies transitions into the Pollards Point formation could also be a factor.

THE EASTERN SEQUENCE

Rocks lying to the east of, and situated structurally above the Long Steady fault, consist mainly of marine sedimentary rocks of the Simms Ridge Formation and the lower part of the Natlins Cove Formation (Heyl, 1937; Betz, 1948; Lock, 1969a, b; Smyth and Schillereff, 1982). The central parts of the sequence are dominated by felsic and mafic volcanic rocks and volcanogenic conglomerate (Figure 3; collectively the Sops Island volcanic member; Heyl, 1937; Betz, 1948; Neale and Nash, 1963). An upper sequence of sandstones overlies the volcanic rocks.

SIMMS RIDGE FORMATION

The Simms Ridge Formation is best exposed along the shores of Sops Arm (Figure 2) and comprises centimetre- to decimetre-scale bedded, variably cleaved, grey to brownish or green shales, siltstone and lesser fine-grained sandstones that contain thin, bioclastic limestone beds. These limestone beds locally contain crinoid stems, coral fragments and rare gastropods and brachiopods (Heyl, 1937; Lock, 1969a) that were interpreted as Mid-Silurian faunas (Lock, 1969b) but have never been formally described. The western, basal contact of the Simms Ridge Formation is best observed along Corner Brook south of Pollards Point where it is a low-angle, east-dipping structure forming part of the Long Steady fault (Kerr, 2006a). In the fault zone, and on the shoreline just east of the mouth of Corner Brook, rocks of the Simms Ridge Formation are muscovite–quartz–ankerite-schists interpreted as tectonized siltstone and sandstone units. These rocks are moderately to strongly cleaved (S_1 foliation = 014/28°E) with variable bedding–cleavage relationships and late refolding of the strong cleavage. Kerr (Plate 11, 2006a) described rootless isoclinal folds within this zone, and suggested that this might provide evidence for a complex early history for the fault zone. The lowermost Simms Ridge Formation, immediately above the Long Steady fault, is the setting for the precious-metal-bearing quartz–ankerite–pyrite–chalcopyrite–galena veins of the Browning Mine. Syn- to posttectonic ankerite porphyroblasts characterize these schists, are spatially associated with the gold mineralization, and have been suggested to be part of the alteration assemblage. The veins postdate the strong regional foliation, are typically massive, but are locally warped, kinked or brecciated. This is the setting of the Ar–Ar geochronology sample (HS09-45B; *see* later discussion).

NATLINS COVE FORMATION

The threefold division of the Natlins Cove Formation of Heyl (1937), further supported by Kerr (2006a), is used herein. This unit, known to be Silurian (Shrock and Twenhofel, 1939; Berry and Boucot, 1970; *see* review in Boyce *et al.*, 1993) consists of siliciclastic sedimentary rocks overlain by volcanic and volcaniclastic rocks, in turn overlain by siliciclastic sedimentary rocks. The contact between the Simms

Ridge and Natlins Cove formations is reported as a conformable transition, marked by the first appearance of thicker sandstone beds (Heyl, 1937; Lock, 1969a). In the north, the Natlins Cove Formation is juxtaposed against the Frenchmans Cove formation, and the Simms Ridge Formation is cut out by the Long Steady fault (Smyth and Schifflereff, 1982; Kerr, 2006a). The sedimentary rocks of the Natlins Cove Formation appear to be east-facing and east-dipping, and may be more openly folded than the underlying Simms Ridge Formation. The difference in deformation state may reflect a significant competency contrast between the Simms Ridge and Natlins Cove formations.

Lower Sedimentary Package

The lower member of the Natlins Cove Formation is dominated by well-bedded, decimetre-scale dark-grey siltstone and buff to locally pink or white sandstone layers. Crossbedding and ripple marks are variably developed in sandstone. Additionally, thin, metre-scale, locally fossiliferous limestone and calcareous sandstone beds also occur in the sequence, and these are discussed by Heyl (1937), Lock (1969a), Berry and Boucot (1970) and reviewed in Boyce *et al.* (1993).

The middle and upper sections of the lower package are composed of thickly bedded quartz sandstones that pass upward into coarser grained rocks including gritty sandstone and fine-grained conglomerate with felsic volcanic clasts. These pass up into cobble- and boulder-conglomerate below the contact with the volcanic rocks. Collectively, observations indicate that the lower Natlins Cove Formation likely formed in a shallow-marine environment, and the coarsening-upward sequence suggests that the depositional basin was being filled.

Middle Volcanic Package (Sops Island Volcanic Member)

The central part of the Natlins Cove Formation is dominated by volcanic rocks of felsic composition, which are best exposed on Sops Island, but also extend southward on the mainland where they are truncated by the Birchy Ridge Fault zone (Figures 2 and 3). These rocks were termed the Sops Island volcanic member (Heyl, 1937; Betz, 1948; Neale and Nash, 1963) or the Sops Island volcanic rocks (Kerr, 2006a). Felsic volcanic rocks are predominant, in particular on Sops Island (Lock, 1969a, b; Kerr, 2006a), but mafic rocks are also common, particularly south of Sops Arm, where basaltic rocks are repetitively intercalated with rhyolite flows, breccias and tuffs as well as polymict conglomerates with felsic volcanic clasts. Textures in the felsic volcanic rocks vary widely and these include massive, flow-banded and autobrecciated, red, red-brown and grey-pink rhyolite (Plate 1C). Ignimbrites and other variably welded fragmental pyroclastic rocks are also common. Kerr (Plate 8, 2006a) describes and illustrates these varied rocks. South of Sops Arm, basalts of the Natlins Cove Formation comprise massive, green chloritic rocks that are commonly vesicular and/or epidote-amygdaloidal (Plate 1D). The volcanic rocks in the Natlins Cove Formation are variable and complex, likely reflecting abrupt lateral facies variations associated with their proximity to individual volcanic centres. Like the volcanic rocks of the Western sequence, volcanic rocks of the Eastern sequence appear to record a subaerial depositional environment; however, thin sandy volcaniclastic units of both mafic and felsic composition indicate that depositional conditions were intermittently subaqueous.

Upper Sedimentary Package

The upper parts of the Natlins Cove Formation are composed of east-dipping and east-facing, monotonous, thinly bedded, fine-grained grey sandstone and minor siltstone similar to the rocks of the lower parts of the formation. Thin calcareous horizons are fossiliferous (Lock, 1969b) and reportedly contain uppermost (Pridoli) Silurian brachiopods and cystoids, although these have never been formally documented, described and classified. The top of the Natlins Cove Formation has not been seen, as the sequence is juxtaposed against sedimentary rocks of the Carboniferous Anguille Group along the Birchy Ridge Fault (Figure 2).

INTRUSIVE ROCKS

Plutonic rocks of the Gull Lake intrusive suite (Smyth and Schillereff, 1982; Saunders and Smyth, 1990) dominate in the south of the area (Figure 2) and consist of a wide variety of rock types including gabbro, trondhjemite, granodiorite and granite. The intrusive rocks have not been precisely dated, but were described as having a poorly defined U–Pb zircon crystallization age of *ca.* 398 Ma (Erdmer, 1986; Tuach, 1987). Field relationships suggest that the emplacement of the Gull Lake intrusive suite postdates most deformation of the Sops Arm group (Smyth and Schillereff, 1982; Saunders and Smyth, 1990), and that it intrudes only the Western sequence of the group. Although major- and selected trace-element lithogeochemical data for these rocks were discussed by Saunders and Smyth (1990), modern, high precision rare-earth element and U–Pb geochronological data are lacking and, as such, they are not discussed further herein.

Minor dykes and sills of felsic composition occur in many units within the Sops Arm group, including the Jackson's Arm, Frenchmans Cove, Simms Ridge (Plate 1E) and

Natlins Cove formations (Plate 1E, F). They have yet to be confirmed in the Pollards Point formation, but a variably mylonitized example cuts tonalite of the Coney Head complex in the Boot and Hammer exploration trench (Reid and Myllyaho, 2012: Figure 2). These buff to pink felsic dykes are typically aphanitic, but locally contain quartz and/or potassium-feldspar phenocrysts. Some are concordant with bedding, particularly in rocks of the Western sequence, but those in the Eastern sequence are more clearly discordant. These intrusions have widely been interpreted as possible feeder dykes to felsic volcanic rocks higher up in the Sops Arm group (Lock, 1969a; Smyth and Schillereff, 1982; Kerr, 2006a).

U–Pb GEOCHRONOLOGY

Two multi-kilogram samples were processed for U–Pb geochronology using standard methods of crushing and mineral separation under clean laboratory conditions. Zircon concentrates were processed as described by Sparkes and Dunning (2014) using the chemical abrasion technique for all analyses; details of zircon morphology and quality are provided in Table 1. Age calculations were performed using the ISOPLOT program (Ludwig, 2008).

SAMPLE HS13-178A

West of the community of Sops Arm, where Highway 420 turns north to Jackson's Arm, the base of the Sops Arm group is well exposed and is in fault contact with strongly deformed schists and marbles of the Cambo-Ordovician platformal sequence (Kerr and Knight, 2004; Kerr, 2006a). Rocks exposed within and immediately above the basal contact are strongly tectonized, and difficult to identify. Approximately 220 m east of the basal contact is a lengthy roadside exposure through the Pollards Point formation. At the western end, the rocks are northeast-trending, steeply to moderately east-dipping polymict conglomerates, containing monzogranite, shale and porphyritic felsic volcanic clasts. This unit is overlain to the east by brecciated, flow-banded and massive rhyolite. A sample of massive grey rhyolite (Plate 2A; HS13-178A; UTM NAD 27 zone 21 506295E - 5513186N; Figure 2) was collected for U–Pb geochronology. Three zircon fractions from this sample (Table 1; Figure 4A), each consisting of a few grains of the highest quality euhedral zircon, plot on top of each other on concordia (Figure 4B), and yield a weighted average $^{206}Pb/^{238}U$ age of 434.3 ± 1.1 Ma (uncertainty at the 95% confidence interval, MSWD = 0.078).

SAMPLE HS13-105B

On the southern shore of Sops Arm, approximately 1 km east of the contact between the Pollards Point and

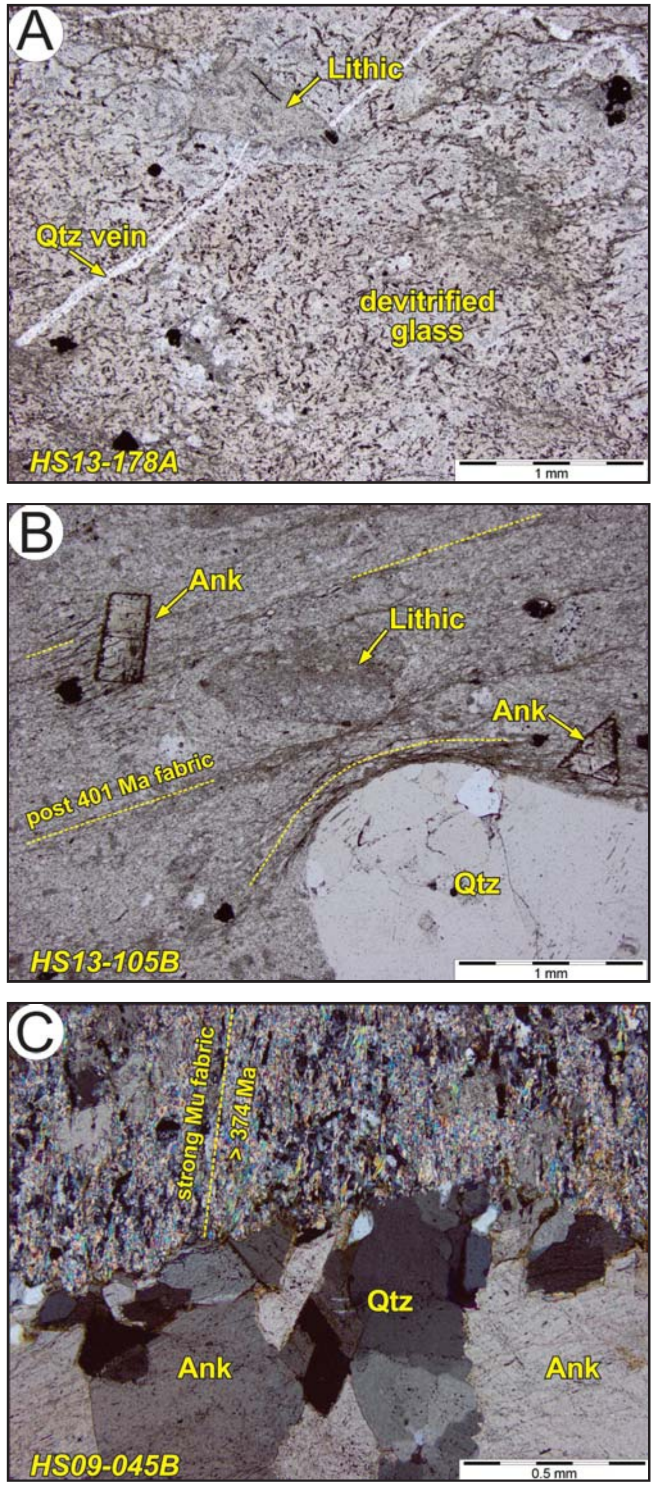

Plate 2. *Photomicrographs of samples analysed by U–Pb and $^{40}Ar–^{39}Ar$ geochronology. A) Rhyolite HS13-178A. B) Rhyolite dyke HS13-105B. Note the spaced cleavage defined by white mica and the euhedral ankerite porphyroblasts. C) Photomicrograph of sample HS09-45B, a muscovite–quartz–albite–ankerite schist that forms the immediate host to an undeformed quartz+chalcopyrite+galena-bearing quartz vein in the immediate footwall of the Browning Mine. Key: Qtz – quartz; Ank – ankerite; Lithic – lithic clast; Mu – muscovite.*

Table 1. U–Pb zircon data for 2 felsic rocks of the Sops Arm group. HS13-178A is a rhyolite flow of the Western sequence (Pollards Point formation) and, HS13-105B is a rhyolite dyke that crosscuts the Simms Ridge Formation of the Eastern sequence

		Concentration	Measured			Corrected Atomic Ratios *							Age [Ma]		
Fraction	Weight [mg]	U [ppm]	Pb rad	total common Pb [pg]	$^{206}Pb/^{204}Pb$	$^{208}Pb/^{206}Pb$	$^{206}Pb/^{238}U$	+/-	$^{207}Pb/^{235}U$	+/-	$^{207}Pb/^{206}Pb$	+/-	$^{206}Pb/^{238}U$	$^{207}Pb/^{235}U$	$^{207}Pb/^{206}Pb$
HS13-178A Rhyolite- Pollards Point formation (UTM NAD 27 zone 21 506295E, 5513186N)															
Z1 4 med euh prm	0.004	275	21.0	4.1	1181	0.2129	0.06973	30	0.5334	46	0.05548	46	435	434	431
Z2 3 med clr euh	0.003	281	21.5	2.1	1800	0.2194	0.06965	30	0.5332	24	0.05552	26	434	434	433
Z3 6 clr med prm	0.006	168	12.7	2.5	2286	0.2080	0.06972	48	0.5313	40	0.05527	34	434	433	423
HS13-105B Rhyolite dyke- Simms Ridge Formation (UTM NAD 27 zone 21 507128E, 5510509N)															
Z1 1 sml clr prm	0.001	428	29.6	3.4	528	0.1974	0.06425	38	0.4800	94	0.05418	98	401	398	379
Z2 1 clr sml prm	0.001	134	9.0	2.2	259	0.1591	0.06431	38	0.4770	116	0.05379	122	402	396	362
Z3 3 clr sml prm	0.003	61	4.1	7.2	121	0.1658	0.06425	38	0.4877	266	0.05505	280	401	403	414
Z4 4 sml clr prm	0.004	296	20.1	2.6	1868	0.1768	0.06413	24	0.4843	20	0.05477	22	401	401	403
Z5 2 clr euh prm	0.002	342	23.4	2.1	1307	0.1835	0.06419	36	0.4805	48	0.05429	46	401	398	383

Notes: Z=zircon, 3,6 =number of grains, clr=clear, med=medium, prm =prism, euh=euhedral.
All zircon was chemically abraded (cf. Mattinson, 2005).
Weights were estimated, and so U and Pb concentrations have large uncertainties.
* Atomic ratios corrected for fractionation, spike, laboratory blank of 1-2 picograms of common lead, and initial common lead at the age of the sample calculated from the model of Stacey and Kramers (1975), and 0.3 picogram U blank. Two sigma uncertainties are reported after the ratios and refer to the final digits.

Simms Ridge formations (Figure 2), moderately inclined, centimetre- to metre-scale bedded, green-grey sandstone and siltstone of the Simms Ridge Formation are transformed to muscovite–chlorite–quartz–albite schists. Bedding and cleavage are subparallel, dipping at around 30 to 35°E. These rocks are crosscut by a ≤2-m-thick dyke of aphanitic, potassium feldspar and quartz porphyritic, orange-pink rhyolite porphyry. The discordance between bedding/cleavage and the margins of the dyke is very slight, but the margins of the dyke preserve a well-developed margin-parallel foliation and a weak cleavage in its interior. Notably, euhedral ankerite porphyroblasts overgrow this cleavage (Plate 2B). A sample of the interior of the dyke (HS13-105B; UTM NAD 27 zone 21 507128E - 5510509N; Figure 2) was collected for U–Pb geochronology. The sample yielded a large amount of high-quality zircon prisms (Figure 4C) and five analyses were undertaken on fractions consisting of 1 to 4 of the clearest euhedral prisms. The data all overlap, having variable to large uncertainties on the $^{207}Pb/^{235}U$ ages, but consistently small uncertainties on the more robust $^{206}Pb/^{238}U$ ages (Figure 4D). The weighted average $^{206}Pb/^{238}U$ age from all five analyses is 401.1 ± 0.8 Ma, at the 95% confidence interval (MSWD = 0.20). This age is clearly distinct from the result obtained from the Sops Arm rhyolite, and resembles the more imprecise U–Pb zircon age determinations for nearby Devonian plutonic rocks of the Gull Lake intrusive suite (Erdmer, 1986).

$^{40}Ar–^{39}Ar$ THERMOCHRONOLOGY

A $^{40}Ar–^{39}Ar$ laser step-heating age was determined for foliation-defining muscovite (250–350 µm grain size), extracted from sample HS09-45B exposed in the immediate footwall of the Browning Mine adit (Figure 2). This sample is a fine-grained, muscovite–quartz–albite–ankerite-bearing schistose siltstone that is cut by a massive pyrite–chalcopyrite±galena-bearing quartz–ankerite vein. A sample of combined schistose host rock and the

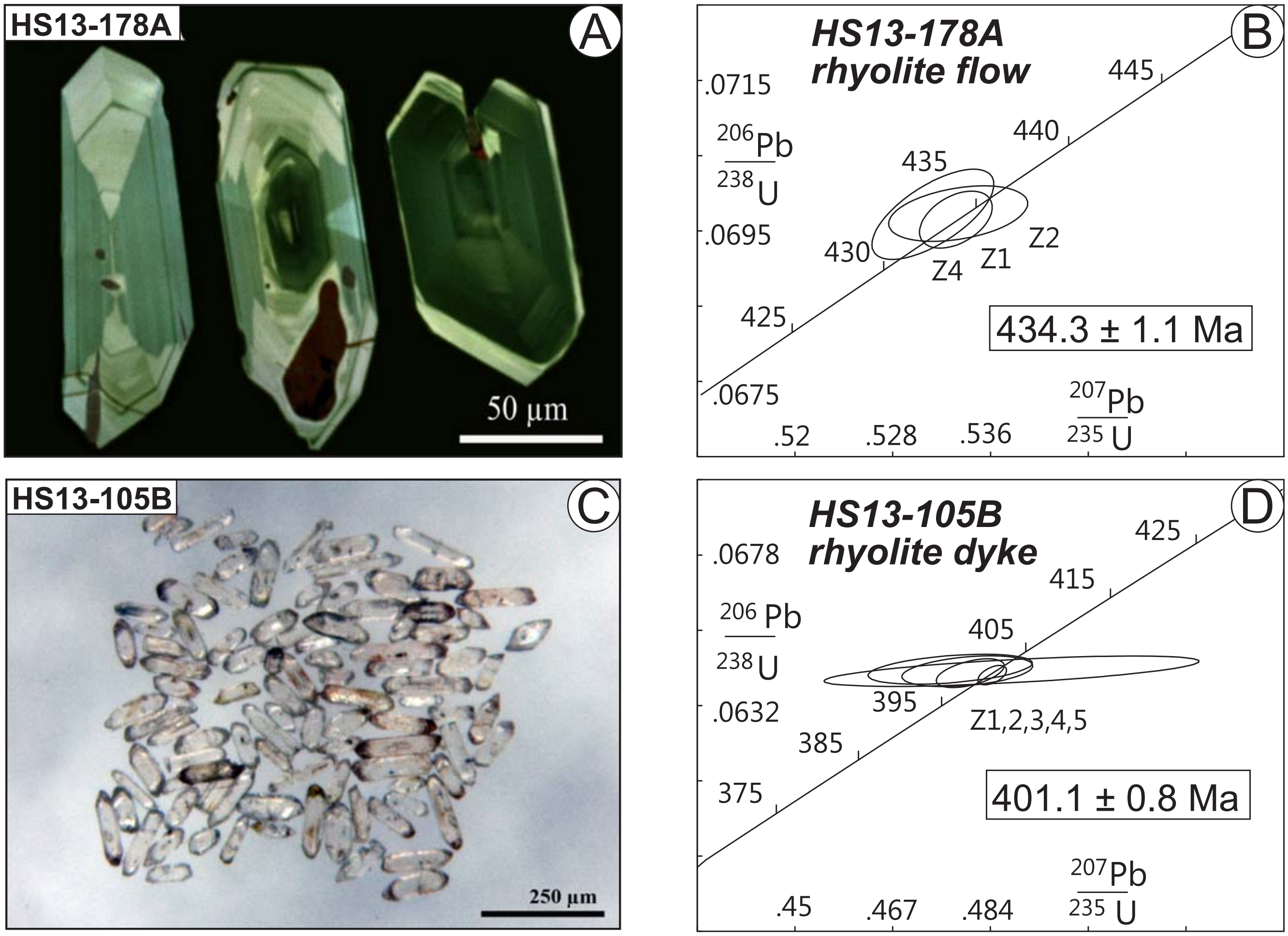

Figure 4. *A) Cathodoluminescence image of high-quality, euhedral zircon prisms from sample HS13-178A. Note the large melt inclusion in the central grain. B) U–Pb concordia diagram of zircon analyses from rhyolite HS13-178A. C) Photomicrograph of representative zircons from the felsic dyke (HS13-105B) that crosscuts the lower siltstones of the Simms Ridge Formation of the Eastern sequence. D) U–Pb concordia diagram of zircon analyses from the felsic dyke HS13-105B.*

quartz–ankerite vein yielded 6.48 ppm Au, 3.88 ppm Ag and, 1695 ppm Cu. The foliation-defining white mica immediately adjacent to the vein (Plate 2C) has been identified as muscovite using visible/infra-red spectrometric analysis (H. Sandeman, unpublished data, 2016). The muscovite in the wall-rock schist is typically ≤400 µm in long dimension and of suitable size to ensure a relatively pure mineral separate. As such, the mineral separate contains only a very small volume of other fine-grained mineral phases. These impurities consist dominantly of albite and minor quartz, which contain no appreciable potassium, and will not contribute radiogenic ^{39}Ar to the step-heating age.

The ^{40}Ar–^{39}Ar age was obtained at Queen's University ^{40}Ar–^{39}Ar Thermochronology Laboratory following the methods of Sandeman and McNicoll (2015). The dates and errors are calculated using the procedure of Dalrymple *et al.* (1981) and the constants of Steiger and Jäger (1977). Plateau and inverse isotope correlation dates are calculated using ISOPLOT v. 3.60 (Ludwig, 2008). A plateau is herein defined as 3 or more contiguous steps containing >50% of the ^{39}Ar released, with a probability of fit >0.01 and MSWD <2. Uncertainties shown in Table 2 and on Figure 5 represent the analytical precision at 2σ, assuming that the uncertainties in the ages of the flux monitors are zero. This is suitable for comparing within-spectrum variation and determining which steps form a plateau (*e.g.*, McDougall and Harrison, 1988, page 89). The gas steps used in the calculation of the plateau age are marked by bold type in Table 2 and by shaded boxes in Figure 5A.

The criteria for a plateau were fully satisfied by the gas-release spectra for sample HS09-45B (Table 2; Figure 5). The muscovite yielded a simple argon release spectrum (Figure 5A). All of the gas release fractions conform to a plateau with the exception of the final, high-temperature release fraction, perhaps indicating extraneous argon released from the grain separate. With the exception of a

Table 2. ^{40}Ar–^{39}Ar thermochronological data for sample HS09-45B, a muscovite–quartz–albite–ankerite schist cut by massive quartz–carbonate–sulphide veins exposed in the immediate footwall of the Browning Mine

Sample	Mineral	J	± (1σ)	% error	Lab #	Int Age (Ma)	± (2σ)	with ± in J
HS09-45B	Muscovite	0.005635	0.000021	0.37	D-725	374.76	0.92	2.69
Can/Pos	222/43							

Plateau Segm.	Plateau Age	± (2σ)	with ± in J	MSWD	% 39Ar	Probability	Initial Ratio	± (1σ)
	373.66	1.29	2.83	0.08	55.04			
IsoPlot PA	374.22	0.80	N/A	0.34	90.00	0.991	N/A	N/A
IsoPlot CA	374.00	2.60	N/A	0.26	90.30	0.998	313	16

Step no	Power (%)	$^{40}Ar/^{39}Ar$	± (1σ)	$^{38}Ar/^{39}Ar$	± (1σ)	Decay corrected true ratios $^{37}Ar/^{39}Ar$	± (1σ)	$^{36}Ar/^{39}Ar$	± (1σ)	$^{40}Ar^*/^{39}Ar(K)$	± (1σ)	$^{40}Ar^*$ (%)	%39Ar	Cumulative ^{39}Ar (%)	Age (Ma)	± (1σ)	Ca/K	± (1σ)	Cl/K	± (1σ)
1	3.0	101.155	1.821	0.211	0.014	0.472	0.041	0.193	0.007	44.293	1.831	43.8	0.2923	0.29	401.98	14.90	0.86	0.08	0.0369	0.00
2	4.0	51.221	0.381	0.087	0.003	4.248	0.070	0.034	0.002	41.539	0.548	80.9	1.0116	1.31	379.43	4.52	7.80	0.38	0.0154	0.00
3	5.0	43.101	0.237	0.029	0.002	6.964	0.064	0.010	0.001	40.859	0.280	94.3	2.3076	3.62	373.83	2.32	12.81	0.61	0.0032	0.00
4	5.7	41.742	0.180	0.020	0.001	3.220	0.028	0.004	0.000	40.971	0.206	97.9	3.3841	7.02	374.75	1.70	5.91	0.28	0.0014	0.00
5	6.2	41.571	0.197	0.014	0.001	2.105	0.018	0.003	0.000	41.019	0.221	98.5	3.1217	10.14	375.14	1.82	3.86	0.18	0.0000	0.00
6	6.7	41.366	0.150	0.013	0.001	0.940	0.014	0.001	0.000	41.114	0.161	99.3	4.7383	14.88	375.92	1.33	1.72	0.08	0.0000	0.00
7	7.1	41.158	0.162	0.012	0.001	0.518	0.012	0.001	0.000	40.939	0.172	99.4	4.6274	19.51	374.48	1.42	0.95	0.05	0.0000	0.00
8	7.5	41.156	0.178	0.012	0.001	0.235	0.007	0.001	0.000	40.889	0.190	99.3	5.2346	24.74	374.07	1.57	0.43	0.02	0.0000	0.00
9	7.8	41.070	0.168	0.012	0.001	0.137	0.005	0.001	0.000	40.856	0.176	99.5	4.3062	29.05	373.80	1.45	0.25	0.01	0.0000	0.00
10	8.2	41.069	0.182	0.012	0.001	0.269	0.007	0.001	0.000	40.852	0.196	99.5	3.9063	32.95	373.76	1.62	0.49	0.03	0.0000	0.00
11	8.7	41.192	0.153	0.013	0.001	0.077	0.004	0.001	0.000	40.822	0.162	99.1	8.9279	41.88	373.51	1.34	0.14	0.01	0.0000	0.00
12	9.2	40.988	0.172	0.012	0.001	0.070	0.004	0.001	0.000	40.778	0.184	99.5	4.0889	45.96	373.15	1.52	0.00	0.01	0.0000	0.00
13	10.0	40.991	0.191	0.012	0.001	0.044	0.003	0.001	0.000	40.800	0.198	99.5	8.5487	54.51	373.33	1.64	0.08	0.01	0.0000	0.00
14	10.8	40.952	0.185	0.012	0.001	0.032	0.004	0.000	0.000	40.798	0.198	99.6	5.1634	59.67	373.32	1.63	0.06	0.01	0.0000	0.00
15	12.0	41.143	0.145	0.012	0.001	0.031	0.003	0.001	0.000	40.925	0.157	99.5	5.0582	64.73	374.36	1.30	0.06	0.01	0.0000	0.00
16	14.0	41.027	0.208	0.012	0.001	0.030	0.003	0.000	0.000	40.868	0.211	99.6	15.0530	79.78	373.90	1.75	0.05	0.01	0.0000	0.00
17	18.0	41.165	0.189	0.012	0.001	0.023	0.002	0.001	0.000	40.976	0.197	99.5	10.5315	90.30	374.79	1.62	0.04	0.00	0.0000	0.00
18	45.0	41.777	0.205	0.014	0.001	0.089	0.006	0.001	0.000	41.571	0.213	99.5	9.6984	100.00	379.70	1.76	0.16	0.01	0.0000	0.00

__Footnotes:__ **The following constants were used. All errors are 1-sigma** **Plateau weighted mean Ca/K = 0.12**

All measurements were made using an MAP-216 mass spectrometer and the same electron multiplier maintained at a gain of 100 over the Faraday.
The same mass spectrometer operating conditions were used for all measurements. 1 mV ~ 4x10-13 cm3 (~1.9x10-17 moles).
Samples were irradiated at the McMaster reactor in position 8C without Cd shielding for 316 MWh. GA-1550 biotite and Hb3Gr hornblende (98.5 and 1074 Ma) were used as a flux monitors.
J values and errors for samples were determined by polynomial fit to replicate analyses of standards at measured positions along the length of the irradiation capsule.
Laser power is expressed as a % of maximum output power of a Merchantek MIR 10-30 CO2 laser (a facetted lens is used to diffuse the beam over 3 mm pits).

Atmospheric Ar ratios: ± (1σ)

38/36Atms =	0.1879	0.0003
40/36Atms =	295.5	0.031
Measured Atmos =	283.18	1.20 used for a linear discrimination correction.

Ratios used to correct for interfering isotopes:

		± (1σ)			± (1σ)			± (1σ)		
40/39K=	0.03020	0.00091	39/37Ca=	0.00070600	0.000028	36/37Ca=	0.00027900	0.00001		
38/39K=	0.01400	0.00000	38/37Ca=	0.00003170	0.000000	36/39Ca=	0.39518	0.020	36/38Cl=	320

Decay Constants Used:
Lambda 40K = 5.543E-10Lambda 39Ar =2.58E-03 (1/a)
Lambda 37Ar = 7.2088 Lambda 36Cl =2.30E-06 (1/a)
Blank corrected 39Ar was decay corrected using f = 1.00051
Both 37Ar and 39Ar decay corrections include the time in the reactor.

Conversion factors:

		± (1s)
ClK fact =	0.23	0.02
CaK fact =	1.83	0.085

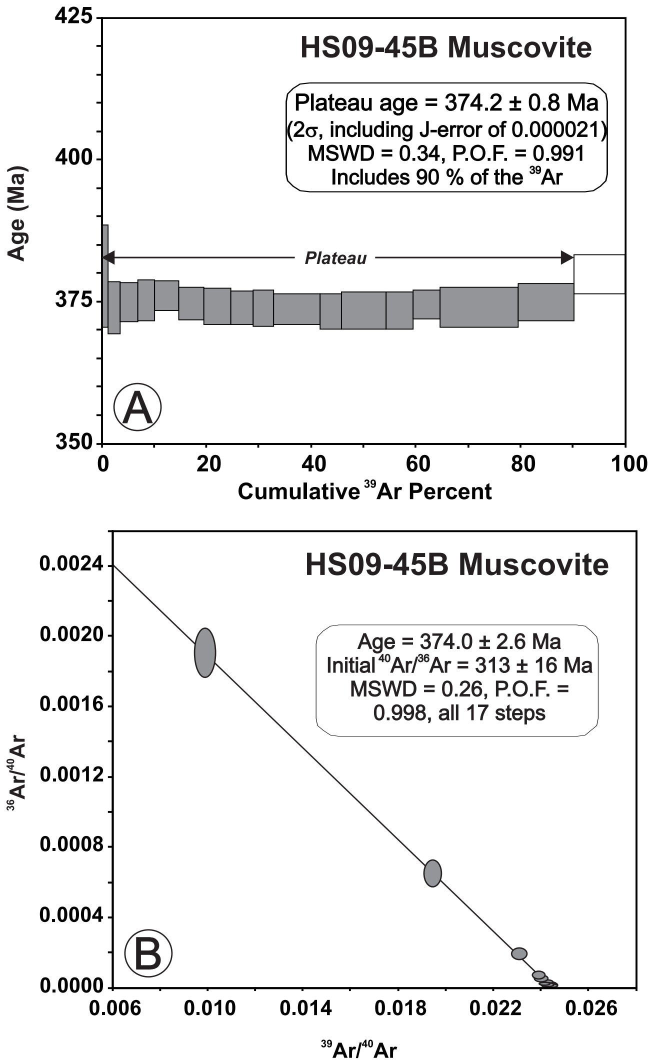

Figure 5. *A) ^{40}Ar–^{39}Ar age spectrum for a muscovite separate from quartz–sericite schist sample HS09-45B. B) Corresponding ^{36}Ar–^{40}Ar vs ^{40}Ar–^{39}Ar inverse isochron diagram.*

large error on the initial, small volume gas fraction, each individual gas fraction is characterized by a relatively small error, thus yielding a plateau age with a correspondingly small error. Gas release steps 2 through 17 yield a plateau age of 374.2 ± 0.8 Ma, representing 90% of the ^{39}Ar released (MSWD = 0.34; POF = 0.991), overlapping, within uncertainty, the total gas integrated age of 374.8 ± 2.7 Ma. Similarly, the gas release steps yield a well-defined inverse isotope correlation age of 374.0 ± 2.6 Ma with an initial ^{40}Ar–^{36}Ar =313 ± 6 and an MSWD of 0.26 (Figure 5B). Thus, the plateau age of 374.2 ± 0.8 Ma is interpreted as the time at which the muscovite cooled through ~ 300°C (McDougall and Harrison, 1988; Reynolds, 1992) and hence, in this situation, the time of cooling of the foliation defining muscovite. The precious-metal-bearing quartz–ankerite veins cut this fabric and are younger than 374 Ma.

PETROCHEMISTRY

ANALYTICAL METHODS

Thirty five lithogeochemical samples were obtained from the Sops Arm group and spatially associated dykes. These include seven felsic volcanic and volcaniclastic rocks from the Eastern and Western sequences, nine variably deformed basaltic rocks of the Western sequence, and seven basaltic rocks of the Eastern sequence. Six felsic dykes and/or sills, three of which cut the Frenchmans Cove formation of the Western sequence, and three of which cut the Simms Ridge Formation of the Eastern sequence were also included. All specimens were submitted for determination of their major-, trace-, rare-earth element (REE) and some for gold pathfinder-element contents (Table 3). Samples were analyzed at the Department of Natural Resources, Government of Newfoundland and Labrador, Geochemical Laboratory (Howley Building, Higgins Line) for their major and trace elements using the methods outlined in Sandeman and McNicoll (2015). The Au, Cd, Bi, As and Sb were determined *via* Instrumental Neutron Activation Analysis (INAA) at Becquerel Laboratories (http://www.becquerellabs.com/) using their standard techniques.

COMMENTS ON ELEMENT MOBILITY AND ALTERATION

Many of these volcanic and volcaniclastic rocks were deposited in subaerial or shallow-marine environments and may have been subjected to extensive weathering. Moreover, the common epidote–quartz amygdaloidal character of the mafic rocks, along with local sericitization of the felsic rocks, in conjunction with the local deformation, indicates that many are at greenschist facies, and caution must be employed in the interpretation of their petrochemistry. Samples show marked variability in their K_2O, Na_2O and loss on ignition (LOI) values and large ion lithophile element (LILE: Rb, Sr, Ba, Cs) abundances. Many plot in the spilite (Na-metasomatised) and keratophyre (K-metasomatised) fields (Hughes, 1973), and exhibit large ranges in their alkali-element contents (Figure 6A, B) or have excessively elevated LOI. Such observations suggest that these elements may have been mobile during deformation and metamorphism. The immobile major and trace elements, along with the high field strength (HFSE) and rare-earth (REE) elements, show more consistent values and systematic behav-

Table 3. Lithogeochemical data for selected volcanic and felsic dyke rocks of the Sops Arm group. All oxides are in weight % whereas trace elements are given in ppm with the exception of Au (ppb). UTM coordinates are in NAD27, Zone 21 format. Key: R – rhyolite; B – basalt; T – tuff; FB – flow-banded; BR – brecciated; Sc – schistose; Q – quartz; K – potassium feldspar; Pl –plagioclase; p – porphyritic; Ep – epidote; amy – amygdaloidal; NCF – Natlins Cove Formation; PPf – Pollards Point formation; FCf – Frenchmans Cove formation; SRf – Simms Ridge Formation. FeO^T – total iron as ferrous iron; negative number = concentration is below the detection limit; -99 = not analyzed; Mg# = molecular ($MgO/MgO+FeO^T$)*100; CN subscript denotes chondrite normalized ratios

Sample	**HS09-046A**	**HS10-070A**	**HS10-070C**	**HS10-081B**	**HS12-192**	**HS12-193**	**HS13-148**	**HS10-077**	**HS10-081A**	**HS12-191A**
Lab Number[1]	8940614	8940783	8940785	8940792	8940726	8940618	8940735	8940421	8940791	8940616
Rock Group	volcanic	volcanic	volcanic	volcanic	volcanic	volcanic	volcanic	volcanic	volcanic	volcanic
Rock-name	R-FB	R-FB	R-FB	R-QKp	RT-Kp	R-BR	R-BR	B-Plp (Ep amy)	B-(Ep amy)	B-(Ep amy)
Statigraphic unit	NCF	NCF	NCF	NCF	NCF	NCF	NCF	NCF	NCF	NCF
Sequence	Eastern	Eastern	Eastern	Eastern	Eastern	Eastern	Eastern	Eastern	Eastern	Eastern
UTM_East	509030	511168	511168	510393	510549	510487	511139	511308	510393	510767
UTM_North	5502684	5509861	5509861	5507292	5499103	5498953	5507063	5507312	5507292	5499389
Mg#	33.10	9.49	4.62	52.45	13.09	28.45	10.82	41.47	45.03	49.93
SiO_2	67.73	77.23	76.55	71.77	77.50	76.97	76.18	49.71	51.21	47.93
TiO_2	0.26	0.18	0.16	0.28	0.15	0.19	0.16	2.86	3.08	3.24
Al_2O_3	14.24	10.43	9.81	11.67	10.44	11.53	10.36	14.66	13.54	14.91
FeO^T	3.80	2.33	2.37	3.43	1.70	1.83	3.12	10.60	11.28	11.96
Fe_2O_3	3.55	2.31	2.28	1.39	1.62	1.54	3.24	6.09	4.62	5.58
FeO	0.61	0.25	0.32	2.18	0.24	0.44	0.20	5.12	7.13	6.94
MnO	0.02	0.00	0.00	0.03	0.01	0.02	0.01	0.16	0.19	0.20
MgO	1.06	0.14	0.06	2.12	0.14	0.41	0.21	4.21	5.19	6.69
CaO	0.03	0.07	0.45	0.49	0.17	0.12	0.07	9.11	5.88	5.74
Na_2O	2.20	0.40	0.55	1.23	5.10	2.52	2.65	4.80	3.02	4.64
K_2O	8.81	6.76	7.74	6.52	0.91	6.06	4.96	0.06	1.85	1.77
P_2O_5	0.00	0.00	0.00	0.03	0.00	0.01	0.01	0.43	0.74	0.49
LOI	0.52	0.48	0.54	0.99	0.44	0.44	0.45	1.78	3.07	1.02
Total	99.08	98.29	98.50	98.94	96.75	100.30	98.53	99.58	100.30	99.93
Ag	1.29	-0.05	-0.05	0.69	-0.05	-0.05	-0.05	-0.05	-0.05	-0.05
As	-99	2.1	3.6	8.4	3.8	-99	-2.0	-2.0	7.8	-99
Au (ppb)	-99	-1	-1	-1	-1	-99	-1	-1	-1	-99
Ba	124	411	344	552	18	173	92	32	227	526
Be	4.7	1.8	1.5	2.6	3.4	2.9	3.7	1.6	1.9	1.2
Bi	-0.4	-0.5	-0.5	-0.5	-0.4	-0.4	-0.4	0.3	-0.5	-0.4
Br	-99	-1	-1	-1	-1	-99	-1	-1	-1	-99
Cd	0.4	-0.2	0.3	-0.2	-0.2	-0.2	-0.2	-0.2	0.2	-0.2
Co	4.0	-1.0	-1.0	2.9	-1.0	1.8	1.0	28.6	23.7	83.6
Cr	-1	2	-1	20	-1	11	-1	80	22	100
Cs	0.9	0.7	0.8	1.2	-0.5	0.7	-0.5	0.1	2.2	2.0
Cu	4	2	3	3	2	4	2	61	4	-1
Ga	36	27	27	47	30	18	29	26	26	20
Ge	3.62	2.52	5.44	16.31	8.24	2.97	4.00	3.72	5.60	4.14
Hf	32.8	18.0	20.4	23.6	19.5	9.3	24.6	5.0	8.2	5.5
In	-0.20	-99	-99	-99	-99	-0.20	-99	0.14	-99	-0.20
Li	19.0	12.7	4.9	36.7	4.6	6.5	2.3	7.8	24.9	20.6
Mn	161	51	47	284	117	143	78	1114	1430	1383
Mo	2	-2	-2	-2	-2	-2	2	2	-2	-2
Nb	49	32	36	38	37	21	57	12	15	12
Ni	5	2	2	13	3	4	4	39	17	56
Pb	3	2	2	3	-1	6	-1	30	18	-1
Rb	220	237	210	158	34	157	118	21	72	51
Sb	-99	0.3	0.3	0.2	0.4	-99	0.4	0.3	0.6	-99
Sc	0.4	0.3	0.3	4.6	0.2	2.1	0.2	36.2	36.1	36.5
Se	-99	-1	-1	-1	-1	-99	-1	-1	-1	-99
Sn	10	6	6	7	3	4	8	2	2	2
Sr	13	10	15	52	10	26	10	363	444	112
Ti	1177	754	513	1855	778	815	1032	18022	18615	15587
Ta	6.07	2.61	2.98	3.04	3.53	2.39	3.80	1.10	1.08	1.08
Th	31.92	15.41	19.40	24.49	19.70	22.72	23.32	4.37	3.59	2.80
Tl	-0.10	0.27	0.31	0.22	-0.10	-0.10	-0.10	-0.10	0.14	-0.10

Table 3. (*continued*) Lithogeochemical data for selected volcanic and felsic dyke rocks of the Sops Arm group. All oxides are in weight % whereas trace elements are given in ppm with the exception of Au (ppb). UTM coordinates are in NAD27, Zone 21 format. Key: R – rhyolite; B – basalt; T – tuff; FB – flow-banded; BR – brecciated; Sc – schistose; Q – quartz; K – potassium feldspar; Pl –plagioclase; p – porphyritic; Ep – epidote; amy – amygdaloidal; NCF – Natlins Cove Formation; PPf – Pollards Point formation; FCf – Frenchmans Cove formation; SRf – Simms Ridge Formation. FeO^T – total iron as ferrous iron; negative number = concentration is below the detection limit; -99 = not analyzed; Mg# = molecular $(MgO/MgO+FeO^T)*100$; CN subscript denotes chondrite normalized ratios

Sample	**HS09-046A**	**HS10-070A**	**HS10-070C**	**HS10-081B**	**HS12-192**	**HS12-193**	**HS13-148**	**HS10-077**	**HS10-081A**	**HS12-191A**
Lab Number[1]	8940614	8940783	8940785	8940792	8940726	8940618	8940735	8940421	8940791	8940616
Rock Group	volcanic	volcanic	volcanic	volcanic	volcanic	volcanic	volcanic	volcanic	volcanic	volcanic
Rock-name	R-FB	R-FB	R-FB	R-QKp	RT-Kp	R-BR	R-BR	B-Plp (Ep amy)	B-(Ep amy)	B-(Ep amy)
Statigraphic unit	NCF	NCF	NCF	NCF	NCF	NCF	NCF	NCF	NCF	NCF
Sequence	Eastern	Eastern	Eastern	Eastern	Eastern	Eastern	Eastern	Eastern	Eastern	Eastern
UTM_East	509030	511168	511168	510393	510549	510487	511139	511308	510393	510767
UTM_North	5502684	5509861	5509861	5507292	5499103	5498953	5507063	5507312	5507292	5499389
Mg#	33.10	9.49	4.62	52.45	13.09	28.45	10.82	41.47	45.03	49.93
U	7.65	2.08	2.48	8.19	4.52	3.62	2.55	1.05	0.90	0.78
V	10.6	13.4	-5.0	25.8	-5.0	14.7	16.1	358.6	305.9	331.0
W	3.6	-1.0	-1.0	-1.0	10.9	1.5	1.8	1.3	-1.0	1.5
Y	102	80	103	97	89	44	133	38	61	35
Zn	52	12	12	72	10	25	20	153	220	210
Zr	1376	918	790	871	841	342	942	224	329	233
La	6.62	13.10	67.04	262.50	100.10	57.65	24.13	25.98	36.47	18.95
Ce	56.62	25.48	137.60	570.00	218.70	123.10	54.50	55.99	82.95	45.26
Pr	1.89	3.02	17.02	67.20	27.74	13.70	7.89	7.20	11.28	6.21
Nd	8.65	11.96	64.77	235.50	110.30	50.79	36.80	32.14	50.94	28.60
Sm	4.17	3.55	14.16	32.85	22.00	9.86	12.37	7.59	11.45	7.34
Eu	0.33	0.39	1.00	1.68	1.29	0.57	0.89	3.06	3.84	2.03
Gd	7.69	5.87	13.95	21.02	19.91	8.54	17.30	7.89	11.95	7.06
Tb	1.80	1.47	2.54	3.17	3.00	1.35	3.31	1.22	1.96	1.20
Dy	15.55	12.04	16.68	17.76	17.63	8.05	23.22	7.83	11.72	7.04
Ho	3.63	2.74	3.61	3.56	3.41	1.60	4.82	1.43	2.28	1.41
Er	12.61	9.20	11.69	10.88	10.31	4.99	15.55	4.34	6.69	3.90
Tm	1.99	1.39	1.69	1.54	1.40	0.71	2.27	0.56	0.91	0.53
Yb	13.99	9.43	11.46	10.40	9.73	5.02	15.41	3.74	5.93	3.70
Lu	2.10	1.40	1.68	1.68	1.44	0.75	2.23	0.54	0.91	0.50
$(La/Yb)_{CN}$	0.34	1.00	4.20	18.10	7.38	8.24	1.12	4.99	4.41	3.68
$(La/Sm)_{CN}$	1.03	2.38	3.06	5.16	2.94	3.77	1.26	2.21	2.06	1.67
$(Gd/Yb)_{CN}$	0.45	0.51	1.01	1.67	1.69	1.41	0.93	1.75	1.67	1.58
Eu/Eu*	0.18	0.26	0.22	0.19	0.19	0.19	0.19	1.21	1.00	0.86
$(Th/Nb)_{CN}$	5.51	4.05	4.54	5.41	4.49	9.32	3.46	3.00	2.01	1.91
$(Th/La)_{CN}$	39.39	9.61	2.36	0.76	1.61	3.22	7.90	1.37	0.80	1.21
$(La/Nb)_{CN}$	0.14	0.42	1.92	7.10	2.79	2.89	0.44	2.18	2.51	1.58

iour for all samples and these provide the firmest basis for petrogenetic interpretation.

ROCK CLASSIFICATION AND MAJOR- AND TRACE-ELEMENT VARIATIONS

Volcanic rocks of the Sops Arm group and crosscutting feslic dykes exhibit a bimodal SiO_2 distribution (Le Bas *et al.*, 1986; Figure 6B). Low-silica samples vary from basalt and basaltic andesite through trachybasalt and basaltic trachyandesite, whereas high-silica samples are dominantly rhyolite with one specimen of trachydacite. The mafic rocks exhibit low Nb/Y, characteristic of subalkaline basalt, and most of the felsic rocks similarly display low Nb/Y, typical of rhyolite, dacite and alkali rhyolite (Pearce, 1996; Figure 6C). The felsic dykes and sills are marginally more alkaline and plot as trachyte and trachyandesite.

In selected major-element, and compatible and incompatible trace-element variation diagrams (*vs* Mg#; Figure 7), the Sops Arm group volcanic rocks and the felsic dykes form a bimodal population in major and compatible trace elements (*e.g.*, SiO_2, TiO_2, FeO^T, CaO, P_2O_5, Cr, Ni). Relative to the mafic volcanic rocks, the felsic rocks have elevated SiO_2 (67.7–80.0 *vs* 38.6–52.5 wt. %), Na_2O (0.40–6.26 *vs* 2.17–4.80 wt. %), K_2O (0.91–8.81 *vs* 0.06–3.50 wt. %), but typically have lower concentrations of

Table 3. (*continued*) Lithogeochemical data for selected volcanic and felsic dyke rocks of the Sops Arm group. All oxides are in weight % whereas trace elements are given in ppm with the exception of Au (ppb). UTM coordinates are in NAD27, Zone 21 format. Key: R – rhyolite; B – basalt; T – tuff; FB – flow-banded; BR – brecciated; Sc – schistose; Q – quartz; K – potassium feldspar; Pl –plagioclase; p – porphyritic; Ep – epidote; amy – amygdaloidal; NCF – Natlins Cove Formation; PPf – Pollards Point formation; FCf – Frenchmans Cove formation; SRf – Simms Ridge Formation. FeO^T – total iron as ferrous iron; negative number = concentration is below the detection limit; -99 = not analyzed; Mg# = molecular $(MgO/MgO+FeO^T)*100$; CN subscript denotes chondrite normalized ratios

Sample	**HS12-191B**	**HS13-144**	**HS13-145**	**HS13-146**	**HS12-205**	**HS13-101**	**HS13-108**	**HS13-109**	**HS13-110**	**HS13-168A**
Lab Number[1]	8940617	8940571	8940572	8940573	8940501	8940667	8940578	8940668	8940566	8940605
Rock Group	volcanic	volcanic	volcanic	volcanic	volcanic	volcanic	volcanic	volcanic	volcanic	volcanic
Rock-name	B-(Ep amy)	B-Sc	B-Sc	B-(Ep amy)	DT-Plp	R-Qp(min)	R-BR	R-Kp	RT-Kp	RT-KQp
Statigraphic unit	NCF	NCF	NCF	NCF	PPf	PPf	PPf	PPf	PPf	PPf
Sequence	Eastern	Eastern	Eastern	Eastern	Western	Western	Western	Western	Western	Western
UTM_East	510767	510362	510760	511177	515276	506268	506644	506900	507250	515052
UTM_North	5499389	5507237	5507162	5507435	5527599	5509815	5511850	5512884	5512711	5525233
Mg#	48.13	41.56	55.31	44.48	17.81	0.00	6.52	6.83	3.61	9.00
SiO_2	46.18	49.68	44.27	45.78	68.48	78.94	69.04	73.59	75.13	79.15
TiO_2	2.98	3.31	2.95	2.69	0.89	0.18	0.41	0.30	0.26	0.16
Al_2O_3	14.20	12.25	14.28	14.69	14.86	9.57	15.25	13.42	11.42	10.30
FeO^T	12.43	12.20	11.79	11.43	2.68	1.61	2.92	1.65	3.12	1.82
Fe_2O_3	6.19	5.11	3.81	4.54	-99	-99	2.71	1.64	3.13	1.71
FeO	6.87	7.61	8.36	7.35	-99	-99	0.48	0.17	0.31	0.28
MnO	0.25	0.18	0.12	0.22	0.11	0.00	0.00	0.01	0.01	0.00
MgO	6.47	4.87	8.19	5.14	0.33	-0.01	0.11	0.07	0.07	0.10
CaO	7.88	5.44	5.61	7.73	0.98	0.02	0.06	0.17	0.21	0.05
Na_2O	3.94	3.65	3.68	2.62	5.41	2.09	3.92	3.96	2.90	0.98
K_2O	0.92	0.99	0.22	2.07	4.12	5.31	6.85	5.71	4.36	5.78
P_2O_5	0.46	0.73	0.44	0.63	0.21	0.01	0.04	0.02	0.02	0.02
LOI	1.11	4.13	5.88	4.20	1.30	1.25	0.54	0.44	0.44	0.37
Total	98.22	98.79	98.74	98.46	99.66	99.17	99.48	99.51	98.29	98.93
Ag	-0.05	-0.05	-0.05	-0.05	-0.05	1.87	-0.05	-0.05	-0.05	-0.05
As	-99	-99	-99	-99	-99	5.3	-99	6.0	-99	-99
Au (ppb)	-99	-99	-99	-99	2	181	-99	-1	-99	-99
Ba	249	108	37	206	771	8840	661	762	296	155
Be	1.1	1.7	1.0	1.3	3.6	1.8	3.2	3.6	3.3	5.0
Bi	1.1	-0.4	-0.4	-0.4	0.2	-0.4	-0.4	-0.4	-0.4	-0.4
Br	-99	-99	-99	-99	-1	-1	-99	-1	-99	-99
Cd	0.2	-0.2	-0.2	-0.2	-0.2	-0.2	-0.2	-0.2	0.3	-0.2
Co	46.9	29.5	43.1	34.8	1.3	0.8	1.6	-1.0	1.4	1.3
Cr	93	5	107	104	-100	2	1	-1	-1	-1
Cs	1.7	1.8	-0.5	3.9	0.7	1.2	1.7	1.4	-0.5	-0.5
Cu	5	-1	63	38	1	98	2	11	19	10
Ga	22	21	21	20	23	28	20	33	27	20
Ge	5.22	4.82	5.23	3.77	6.04	3.93	4.00	6.41	4.20	3.43
Hf	5.0	6.1	4.7	5.2	11.9	24.34	14.5	17.6	19.0	14.4
In	-0.20	-0.20	-0.20	-0.20	-0.10	-99	-0.20	-99	-0.20	-0.20
Li	13.2	22.1	23.3	24.8	10.9	-0.1	4.6	1.7	1.8	1.1
Mn	1756	1231	800	1480	761	21	50	67	87	36
Mo	-2	2	3	2	-1	2	2	-2	2	2
Nb	10	13	11	12	22	41	25	32	31	32
Ni	49	14	46	41	3	4	4	3	5	4
Pb	2	19	-1	19	-1	319	4	16	29	10
Rb	31	50	13	111	110	151	134	172	161	136
Sb	-99	-99	-99	-99	0.6	2.7	-99	1.5	-99	-99
Sc	34.7	36.7	37.7	37.4	13.1	0.4	8.7	4.2	1.4	1.2
Se	-99	-99	-99	-99	-1	-1	-99	-1	-99	-99
Sn	2	2	2	2	3	8	5	6	8	6
Sr	202	233	118	381	90	278	35	40	25	30
Ti	15065	12371	18190	13130	3415	836	1828	1756	1094	786
Ta	0.94	1.35	1.11	1.21	1.41	3.52	2.84	2.40	2.66	2.67
Th	2.73	2.92	1.41	1.23	9.59	20.52	13.58	14.52	14.65	18.43
Tl	-0.10	-0.10	-0.10	-0.10	-0.10	0.74	-0.10	0.65	-0.10	-0.10

Table 3. (*continued*) Lithogeochemical data for selected volcanic and felsic dyke rocks of the Sops Arm group. All oxides are in weight % whereas trace elements are given in ppm with the exception of Au (ppb). UTM coordinates are in NAD27, Zone 21 format. Key: R – rhyolite; B – basalt; T – tuff; FB – flow-banded; BR – brecciated; Sc – schistose; Q – quartz; K – potassium feldspar; Pl –plagioclase; p – porphyritic; Ep – epidote; amy – amygdaloidal; NCF – Natlins Cove Formation; PPf – Pollards Point formation; FCf – Frenchmans Cove formation; SRf – Simms Ridge Formation. FeO^T – total iron as ferrous iron; negative number = concentration is below the detection limit; -99 = not analyzed; Mg# = molecular ($MgO/MgO+FeO^T$)*100; CN subscript denotes chondrite normalized ratios

Sample	**HS12-191B**	**HS13-144**	**HS13-145**	**HS13-146**	**HS12-205**	**HS13-101**	**HS13-108**	**HS13-109**	**HS13-110**	**HS13-168A**
Lab Number[1]	8940617	8940571	8940572	8940573	8940501	8940667	8940578	8940668	8940566	8940605
Rock Group	volcanic	volcanic	volcanic	volcanic	volcanic	volcanic	volcanic	volcanic	volcanic	volcanic
Rock-name	B-(Ep amy)	B-Sc	B-Sc	B-(Ep amy)	DT-Plp	R-Qp(min)	R-BR	R-Kp	RT-Kp	RT-KQp
Statigraphic unit	NCF	NCF	NCF	NCF	PPf	PPf	PPf	PPf	PPf	PPf
Sequence	Eastern	Eastern	Eastern	Eastern	Western	Western	Western	Western	Western	Western
UTM_East	510767	510362	510760	511177	515276	506268	506644	506900	507250	515052
UTM_North	5499389	5507237	5507162	5507435	5527599	5509815	5511850	5512884	5512711	5525233
Mg#	48.13	41.56	55.31	44.48	17.81	0.00	6.52	6.83	3.61	9.00
U	0.75	1.32	0.53	0.50	3.51	4.57	3.88	3.59	4.56	4.42
V	355.9	320.1	361.0	280.1	23.8	9.1	15.8	-5.0	15.9	13.8
W	1.4	1.7	1.3	2.1	1.3	9.9	5.5	1.6	2.0	2.1
Y	39	48	33	42	56	124	55	72	81	77
Zn	207	385	130	160	30	14	22	23	39	19
Zr	215	249	200	221	518	1055	608	704	767	527
La	22.27	25.87	17.78	22.46	61.44	39.40	70.00	76.86	76.13	74.52
Ce	50.55	57.97	39.50	49.80	128.80	82.23	132.60	164.40	171.00	147.40
Pr	6.98	7.88	5.53	7.10	15.61	10.73	17.18	19.95	19.77	19.65
Nd	32.49	36.76	25.60	32.85	63.61	42.18	65.31	77.47	77.30	76.46
Sm	7.83	8.93	6.34	8.21	12.30	10.26	11.60	15.38	15.17	17.32
Eu	2.83	2.88	2.24	2.65	3.37	0.75	1.44	2.75	1.21	0.39
Gd	8.50	9.93	6.73	8.79	11.20	13.55	10.18	14.02	13.77	15.84
Tb	1.32	1.53	1.14	1.30	1.83	2.87	1.66	2.20	2.22	2.54
Dy	7.69	9.58	6.51	8.13	11.21	20.84	10.18	13.51	13.67	15.16
Ho	1.48	1.87	1.32	1.53	2.06	4.63	2.14	2.75	2.77	2.89
Er	4.12	5.44	3.76	4.50	6.36	14.25	6.68	8.35	8.96	8.32
Tm	0.56	0.75	0.49	0.63	0.89	2.06	0.95	1.09	1.27	1.16
Yb	3.61	4.84	3.23	4.15	5.80	13.34	6.79	8.06	8.83	7.71
Lu	0.55	0.73	0.50	0.61	0.93	1.98	1.01	1.20	1.31	1.06
$(La/Yb)_{CN}$	4.43	3.84	3.95	3.88	7.60	2.12	7.40	6.84	6.19	6.93
$(La/Sm)_{CN}$	1.84	1.87	1.81	1.77	3.22	2.48	3.90	3.23	3.24	2.78
$(Gd/Yb)_{CN}$	1.95	1.70	1.72	1.75	1.60	0.84	1.24	1.44	1.29	1.70
Eu/Eu*	1.06	0.93	1.05	0.95	0.88	0.19	0.41	0.57	0.26	0.07
$(Th/Nb)_{CN}$	2.20	1.98	1.13	0.87	3.66	4.24	4.58	3.84	4.05	4.84
$(Th/La)_{CN}$	1.00	0.92	0.65	0.45	1.28	4.26	1.59	1.54	1.57	2.02
$(La/Nb)_{CN}$	2.20	2.14	1.75	1.93	2.87	1.00	2.89	2.49	2.58	2.40

the other major and compatible trace elements (*e.g.*, CaO = 0.05–0.98 *vs* 4.61–9.56 wt%; P_2O_5 = 0.00–0.21 *vs* 0.19–1.61 wt %; Cr = 1.4–19.6 *vs* 4.7–253 ppm) (Figure 7). However, the felsic volcanic rocks typically have higher concentrations of incompatible trace elements, with the exceptions of Sr, Cs and Eu, which are strongly controlled by feldspar fractionation. The felsic dykes have major-element and compatible trace-element contents comparable to those of the felsic volcanic rocks, but have lower abundances of many incompatible trace elements such as Zr, Y, and Yb (Figures 7 and 8D).

The paleotectonic setting of the rocks is evaluated using well-established major- and trace-element discrimination diagrams. The basaltic rocks of both sequences are transitional to calc-alkaline in the Th/Yb *vs* Zr/Y plot (Figure 8A) of Ross and Bedard (2009). They exhibit moderate to elevated TiO_2 at moderate V contents (Figure 8B; Shervais, 1982), and are similar to the basaltic rocks of the possibly correlative Springdale Group of western Newfoundland (Coyle, 1990), but distinct from oceanic basalts of the Mariana Arc (Elliott *et al.*, 1997) and shoshonitic basalts of the Oligocene Andean Arc (Sandeman, 1995). They are within-plate basalts in terms of their Zr and Y variations (Figure 8C; Pearce and Norry, 1979), and again resemble basalts of the Springdale Group, approaching the Zr/Y ratios of the alkaline volcanic rocks of the East African Rift (Chakrabarti *et al.*, 2009). In the Rb *vs* Y+Nb tectonic discrimination

Table 3. (*continued*) Lithogeochemical data for selected volcanic and felsic dyke rocks of the Sops Arm group. All oxides are in weight % whereas trace elements are given in ppm with the exception of Au (ppb). UTM coordinates are in NAD27, Zone 21 format. Key: R – rhyolite; B – basalt; T – tuff; FB – flow-banded; BR – brecciated; Sc – schistose; Q – quartz; K – potassium feldspar; Pl –plagioclase; p – porphyritic; Ep – epidote; amy – amygdaloidal; NCF – Natlins Cove Formation; PPf – Pollards Point formation; FCf – Frenchmans Cove formation; SRf – Simms Ridge Formation. FeO^T – total iron as ferrous iron; negative number = concentration is below the detection limit; -99 = not analyzed; Mg# = molecular ($MgO/MgO+FeO^T$)*100; CN subscript denotes chondrite normalized ratios

Sample	**HS13-167A**	**HS09-056A**	**HS13-116**	**HS13-122A**	**HS13-127**	**HS13-140**	**HS13-155B**	**HS13-166A**	**HS13-174**	**HS09-052B**
Lab Number[1]	8940604	8940758	8940596	8940597	8940622	8940673	8940601	8940575	8940607	8940824
Rock Group	volcanic	volcanic	volcanic	volcanic	volcanic	volcanic	volcanic	volcanic	volcanic	dyke
Rock-name	B	B-Sc (Ep amy)	B-Sc	B-Sc	B-Sc (Ep amy)	B-Sc (Ep amy)	B-Sc	B-Sc	B	R-BR
Statigraphic unit	PPf	PPf	PPf	PPf	PPf	PPf	PPf	PPf	PPf	SRf
Sequence	Western	Western	Western	Western	Western	Western	Western	Western	Western	Eastern
UTM_East	515468	503951	507647	512908	512903	505986	515973	515711	513584	506950
UTM_North	5525384	5508272	5512829	5523403	5522891	5510202	5527891	5527686	5525028	5500775
Mg#	39.54	26.75	51.18	51.07	36.79	66.11	51.55	59.86	54.30	20.32
SiO_2	50.56	47.45	38.62	48.93	48.70	46.58	43.46	44.48	52.54	75.59
TiO_2	2.83	2.45	1.98	1.95	3.32	1.44	1.64	1.28	1.48	0.06
Al_2O_3	13.01	14.67	13.82	15.31	13.02	16.84	16.29	15.22	16.13	13.46
FeO^T	11.49	6.09	11.00	9.75	12.26	9.34	9.34	9.70	8.37	0.70
Fe_2O_3	4.95	3.16	5.74	4.06	5.55	2.61	4.94	1.28	4.09	0.40
FeO	7.04	3.25	5.84	6.10	7.27	6.99	4.90	8.55	4.70	0.34
MnO	0.29	0.17	0.20	0.15	0.26	0.16	0.29	0.14	0.17	0.01
MgO	4.22	1.25	6.47	5.71	4.00	10.22	5.58	8.12	5.58	0.10
CaO	5.46	9.56	6.98	6.75	7.96	5.94	6.59	4.61	5.24	0.07
Na_2O	4.39	2.32	2.41	3.53	2.17	3.18	3.26	3.33	4.52	4.25
K_2O	0.35	3.50	2.09	1.70	1.26	1.26	2.07	0.33	2.07	4.34
P_2O_5	1.57	0.73	0.25	0.33	1.61	0.21	0.23	0.19	0.30	0.01
LOI	3.43	9.15	12.98	3.28	2.40	4.39	8.66	10.05	2.44	0.70
Total	98.87	98.02	98.05	98.48	98.32	100.59	98.44	98.54	99.78	99.36
Ag	-0.05	-0.05	-0.05	0.08	-0.05	-0.05	-0.05	0.07	0.05	-0.05
As	-99	4.5	-99	-99	-99	14.4	-99	-99	-99	2.5
Au (ppb)	-99	-1	-99	-99	-99	-1	-99	-99	-99	-1
Ba	218	415	185	347	1880	288	395	121	941	441
Be	1.3	3.0	1.4	1.5	1.2	0.7	1.8	0.5	1.5	2.0
Bi	0.8	-0.4	1.0	1.3	-0.4	-0.4	0.5	-0.4	0.7	-0.5
Br	-99	-1	-99	-99	-99	-1	-99	-99	-99	-1
Cd	0.2	-0.2	0.3	0.3	-0.2	-0.2	-0.2	-0.2	-0.2	-0.2
Co	16.0	18.2	37.6	38.3	22.7	46.1	38.9	47.1	32.0	-1.0
Cr	-1	6	140	18	-1	253	252	92	90	2
Cs	-0.5	2.6	2.4	2.5	0.6	2.7	1.6	-0.5	0.9	0.9
Cu	-1	20	3	24	4	6	5	7	41	4
Ga	21	24	18	20	21	19	16	16	18	17
Ge	4.80	4.16	4.36	4.15	4.30	4.05	3.76	3.21	3.41	1.00
Hf	6.0	7.2	4.2	5.4	5.4	3.0	3.2	2.5	4.9	2.1
In	-0.20	-99	-0.20	-0.20	-0.20	-99	-0.20	-0.20	-0.20	-99
Li	14.9	15.9	32.5	20.4	20.2	44.2	23.3	42.0	12.7	4.8
Mn	2131	1335	1437	1034	1732	1092	2110	989	1255	66
Mo	-2	3	-2	-2	5	-2	-2	-2	-2	-2
Nb	12	13	7	8	11	8	3	6	10	10
Ni	13	16	71	41	15	90	123	85	70	2
Pb	-1	13	3	4	-1	8	2	-1	5	7
Rb	15	118	85	63	49	46	62	11	48	107
Sb	-99	1	-99	-99	-99	1.6	-99	-99	-99	0.2
Sc	32.4	25.6	26.7	30.1	40.8	37.3	29.9	26.8	20.7	2.3
Se	-99	-1	-99	-99	-99	-1	-99	-99	-99	-1
Sn	2	2	2	1	2	1	1	1	1	1
Sr	158	302	210	402	534	378	112	92	259	127
Ti	15867	11027	3461	12364	20126	8908	4360	2360	8478	351
Ta	1.13	-0.50	-0.50	0.52	1.28	-0.50	-0.50	-0.50	0.79	1.21
Th	4.03	5.87	1.99	3.54	3.60	2.11	1.38	1.07	4.27	9.60
Tl	-0.10	0.37	-0.10	-0.10	-0.10	-0.10	-0.10	-0.10	-0.10	0.20

Table 3. (*continued*) Lithogeochemical data for selected volcanic and felsic dyke rocks of the Sops Arm group. All oxides are in weight % whereas trace elements are given in ppm with the exception of Au (ppb). UTM coordinates are in NAD27, Zone 21 format. Key: R – rhyolite; B – basalt; T – tuff; FB – flow-banded; BR – brecciated; Sc – schistose; Q – quartz; K – potassium feldspar; Pl –plagioclase; p – porphyritic; Ep – epidote; amy – amygdaloidal; NCF – Natlins Cove Formation; PPf – Pollards Point formation; FCf – Frenchmans Cove formation; SRf – Simms Ridge Formation. FeO^T – total iron as ferrous iron; negative number = concentration is below the detection limit; -99 = not analyzed; Mg# = molecular ($MgO/MgO+FeO^T$)*100; CN subscript denotes chondrite normalized ratios

Sample	**HS13-167A**	**HS09-056A**	**HS13-116**	**HS13-122A**	**HS13-127**	**HS13-140**	**HS13-155B**	**HS13-166A**	**HS13-174**	**HS09-052B**
Lab Number[1]	8940604	8940758	8940596	8940597	8940622	8940673	8940601	8940575	8940607	8940824
Rock Group	volcanic	volcanic	volcanic	volcanic	volcanic	volcanic	volcanic	volcanic	volcanic	dyke
Rock-name	B	B-Sc (Ep amy)	B-Sc	B-Sc	B-Sc (Ep amy)	B-Sc (Ep amy)	B-Sc	B-Sc	B	R-BR
Statigraphic unit	PPf	PPf	PPf	PPf	PPf	PPf	PPf	PPf	PPf	SRf
Sequence	Western	Western	Western	Western	Western	Western	Western	Western	Western	Eastern
UTM_East	515468	503951	507647	512908	512903	505986	515973	515711	513584	506950
UTM_North	5525384	5508272	5512829	5523403	5522891	5510202	5527891	5527686	5525028	5500775
Mg#	39.54	26.75	51.18	51.07	36.79	66.11	51.55	59.86	54.30	20.32
U	1.14	1.53	0.46	0.74	1.06	0.41	1.26	0.20	1.49	1.83
V	142.0	189.9	194.0	242.6	205.2	238.4	232.5	206.6	167.3	30.9
W	1.9	-1.0	-1.0	-1.0	5.5	-1.0	-1.0	-1.0	-1.0	-1.0
Y	52	44	30	31	46	25	21	20	25	7
Zn	111	145	95	99	116	167	131	103	79	21
Zr	248	276	178	219	224	109	122	89	214	47
La	35.19	40.86	15.76	26.47	35.73	14.43	16.10	12.65	26.84	9.32
Ce	84.23	86.53	33.75	55.76	83.11	29.63	29.99	26.10	54.39	13.54
Pr	11.77	11.15	4.73	7.10	11.50	4.17	4.25	3.54	6.79	1.17
Nd	53.74	46.88	20.88	30.56	53.02	17.75	18.17	16.17	26.74	4.01
Sm	12.65	10.08	5.46	6.72	11.92	4.18	4.40	3.71	5.55	1.11
Eu	4.05	3.12	1.53	2.09	6.90	1.37	1.35	1.20	1.49	0.28
Gd	12.17	9.94	5.87	6.92	11.75	4.84	4.56	3.77	5.34	1.02
Tb	1.85	1.48	0.93	1.08	1.71	0.79	0.73	0.65	0.80	0.21
Dy	10.66	8.79	5.59	6.33	10.01	4.97	3.87	3.86	4.96	1.35
Ho	1.96	1.63	1.09	1.21	1.80	1.00	0.81	0.81	0.94	0.26
Er	5.59	4.83	3.46	3.46	4.87	2.91	2.30	2.26	2.81	0.77
Tm	0.71	0.64	0.48	0.46	0.62	0.42	0.33	0.30	0.38	0.13
Yb	4.65	4.21	3.03	3.30	4.09	2.87	2.12	2.12	2.49	0.82
Lu	0.66	0.62	0.44	0.44	0.61	0.41	0.30	0.29	0.40	0.13
$(La/Yb)_{CN}$	5.42	6.97	3.73	5.75	6.27	3.61	5.46	4.29	7.74	8.18
$(La/Sm)_{CN}$	1.80	2.62	1.86	2.54	1.94	2.23	2.36	2.20	3.12	5.42
$(Gd/Yb)_{CN}$	2.16	1.96	1.60	1.73	2.38	1.39	1.78	1.47	1.78	1.03
Eu/Eu*	1.00	0.95	0.83	0.94	1.78	0.93	0.92	0.98	0.83	0.81
$(Th/Nb)_{CN}$	2.74	3.90	2.27	3.78	2.74	2.31	3.39	1.39	3.69	8.18
$(Th/La)_{CN}$	0.94	1.17	1.03	1.09	0.82	1.19	0.70	0.69	1.30	8.42
$(La/Nb)_{CN}$	2.93	3.33	2.21	3.45	3.33	1.93	4.84	2.02	2.84	0.97

plot (Figure 8D; Pearce *et al.*, 1984), the felsic volcanic rocks of the Sops Arm group plot in the within-plate portion of the diagram, whereas the felsic dykes plot in the volcanic-arc field.

The nature of the mantle source and the role of continental crust in the origin of the basaltic rocks are evaluated in Figure 9 (Pearce, 2008). The Th/Yb *vs* Nb/Yb and TiO_2/Yb *vs* Nb/Yb plots demonstrate that the Sops Arm group rocks from the Western and Eastern sequences are very similar, having Nb/Yb ratios typical of enriched mid-ocean ridge basalt (EMORB) magmas. Their elevated Th/Yb ratios and curved trends (Figure 9A) are indicative of their chemical variation having resulted from assimilation–fractional crystallization processes involving the middle or upper crust. High TiO_2/Yb ratios relative to the MORB array, suggest that they were derived from melting at depths deeper than that required for the generation of MORB (Pearce, 2008). The origin of the felsic rocks is explored in a $(La/Yb)_{CN}$ *vs* Yb_{CN} plot (subscript CN denotes chondrite-normalized to values of Sun and McDonough, 1989; Figure 9C). This demonstrates that the felsic dykes are characterized by low Yb_{CN} but have moderate to elevated $(La/Yb)_{CN}$ characteristic of silicic melts that have been derived through either fractional crystallization of hornblende and plagioclase from a tonalitic liquid or, partial melting of garnet and/or (?) hornblende-bearing lower crust. In contrast, the felsic volcanic rocks have elevated Yb_{CN} but low $(La/Yb)_{CN}$, characteristic of silicic melts that have been

Table 3. (*continued*) Lithogeochemical data for selected volcanic and felsic dyke rocks of the Sops Arm group. All oxides are in weight % whereas trace elements are given in ppm with the exception of Au (ppb). UTM coordinates are in NAD27, Zone 21 format. Key: R – rhyolite; B – basalt; T – tuff; FB – flow-banded; BR – brecciated; Sc – schistose; Q – quartz; K – potassium feldspar; Pl –plagioclase; p – porphyritic; Ep – epidote; amy – amygdaloidal; NCF – Natlins Cove Formation; PPf – Pollards Point formation; FCf – Frenchmans Cove formation; SRf – Simms Ridge Formation. FeO^T – total iron as ferrous iron; negative number = concentration is below the detection limit; -99 = not analyzed; Mg# = molecular ($MgO/MgO+FeO^T$)*100; CN subscript denotes chondrite normalized ratios

Sample	**HS13-105B**	**HS10-087**	**HS13-121A**	**HS13-121B**	**HS13-185**
Lab Number[1]	8940563	8940793	8940567	8940568	8940587
Rock Group	dyke	dyke	dyke	dyke	dyke
Rock-name	R-KQp	R-QKp	R-PlQp	R-PlQp	R-Plp
Statigraphic unit	SRf	SRf	FCf	FCf	FCf
Sequence	Eastern	Eastern	Western	Western	Western
UTM_East	507128	505377	515603	515598	518138
UTM_North	5510509	5502658	5523461	5523412	5526888
Mg#	37.35	24.45	18.92	39.14	22.12
SiO_2	71.06	73.60	77.43	73.40	75.47
TiO_2	0.25	0.06	0.07	0.07	0.11
Al_2O_3	14.27	14.36	13.49	14.84	13.44
FeO^T	1.84	0.72	0.66	1.26	0.89
Fe_2O_3	1.41	0.55	0.36	1.03	0.82
FeO	0.57	0.22	0.34	0.33	0.16
MnO	0.04	0.04	0.02	0.00	0.01
MgO	0.61	0.13	0.09	0.45	0.14
CaO	0.80	0.44	0.33	0.03	0.31
Na_2O	5.64	6.26	4.34	5.88	3.50
K_2O	1.96	1.37	3.16	1.94	3.43
P_2O_5	0.09	0.02	0.00	0.01	0.02
LOI	1.95	1.19	0.97	0.93	1.00
Total	98.72	98.28	100.63	98.96	98.41
Ag	-0.05	-0.05	0.13	0.18	0.12
As	-99	2.0	-99	-99	-99
Au (ppb)	-99	-1	-99	-99	-99
Ba	513	450	113	131	602
Be	2.1	2.4	2.6	2.8	2.1
Bi	-0.4	-0.5	-0.4	-0.4	-0.4
Br	-99	-1	-99	-99	-99
Cd	-0.2	-0.2	-0.2	-0.2	-0.2
Co	3.4	-1.0	0.8	2.1	2.9
Cr	4	-1	-1	-1	-1
Cs	1.7	0.6	0.7	-0.5	-0.5
Cu	7	3	5	127	6
Ga	18	19	19	25	14
Ge	1.69	1.70	1.78	1.46	1.70
Hf	4.1	2.5	3.3	3.9	3.1
In	-0.20	-99	-0.20	-0.20	-0.20
Li	10.1	0.6	3.5	10.5	2.7
Mn	275	369	192	39	92
Mo	-2	-2	4	3	4
Nb	7	11	20	15	8
Ni	5	1	2	4	3
Pb	7	2	94	13	9
Rb	54	41	61	41	81
Sb	-99	-0.1	-99	-99	-99
Sc	3.1	2.5	3.1	3.0	2.0
Se	-99	-1	-99	-99	-99
Sn	1	1	2	2	2
Sr	85	68	33	16	64
Ti	1159	410	377	441	680
Ta	0.88	1.09	2.73	2.70	0.96
Th	16.39	13.00	23.27	26.89	20.86
Tl	-0.10	-0.50	0.12	-0.10	-0.10

Table 3. (*continued*) Lithogeochemical data for selected volcanic and felsic dyke rocks of the Sops Arm group. All oxides are in weight % whereas trace elements are given in ppm with the exception of Au (ppb). UTM coordinates are in NAD27, Zone 21 format. Key: R – rhyolite; B – basalt; T – tuff; FB – flow-banded; BR – brecciated; Sc – schistose; Q – quartz; K – potassium feldspar; Pl –plagioclase; p – porphyritic; Ep – epidote; amy – amygdaloidal; NCF – Natlins Cove Formation; PPf – Pollards Point formation; FCf – Frenchmans Cove formation; SRf – Simms Ridge Formation. FeO^T – total iron as ferrous iron; negative number = concentration is below the detection limit; -99 = not analyzed; Mg# = molecular ($MgO/MgO+FeO^T$)*100; CN subscript denotes chondrite normalized ratios

Sample	**HS13-105B**	**HS10-087**	**HS13-121A**	**HS13-121B**	**HS13-185**
Lab Number[1]	8940563	8940793	8940567	8940568	8940587
Rock Group	dyke	dyke	dyke	dyke	dyke
Rock-name	R-KQp	R-QKp	R-PlQp	R-PlQp	R-Plp
Statigraphic unit	SRf	SRf	FCf	FCf	FCf
Sequence	Eastern	Eastern	Western	Western	Western
UTM_East	507128	505377	515603	515598	518138
UTM_North	5510509	5502658	5523461	5523412	5526888
Mg#	37.35	24.45	18.92	39.14	22.12
U	3.27	6.77	4.91	22.64	2.95
V	22.5	-5.0	14.0	12.8	12.6
W	1.1	-1.0	6.2	3.2	3.4
Y	10	11	11	15	6
Zn	40	39	32	28	19
Zr	157	56	69	79	103
La	37.63	23.23	11.47	10.67	45.53
Ce	67.96	38.01	20.86	21.84	77.34
Pr	6.92	4.43	2.44	2.72	7.50
Nd	22.79	15.56	9.39	9.82	24.08
Sm	3.36	2.97	2.10	2.42	3.23
Eu	0.82	0.61	0.36	0.46	0.64
Gd	2.43	2.40	2.09	2.67	1.82
Tb	0.32	0.37	0.35	0.47	0.23
Dy	1.76	1.78	2.01	2.60	1.07
Ho	0.32	0.36	0.34	0.48	0.19
Er	0.99	1.10	1.02	1.22	0.63
Tm	0.13	0.15	0.14	0.18	0.07
Yb	0.91	1.07	1.06	1.26	0.60
Lu	0.12	0.14	0.11	0.18	0.09
$(La/Yb)_{CN}$	29.76	15.65	7.78	6.10	54.43
$(La/Sm)_{CN}$	7.23	5.05	3.53	2.85	9.10
$(Gd/Yb)_{CN}$	2.22	1.86	1.63	1.76	2.50
Eu/Eu*	0.88	0.70	0.53	0.55	0.81
$(Th/Nb)_{CN}$	20.32	10.36	9.93	15.40	22.19
$(Th/La)_{CN}$	3.56	4.57	16.58	20.60	3.74
$(La/Nb)_{CN}$	5.71	2.27	0.60	0.75	5.93

derived through fractional crystallization of biotite, plagioclase and potassium feldspar from an intermediate magma.

The rare-earth element (REE) and incompatible trace-element abundances of the rocks are displayed as chondrite-normalized REE (Sun and McDonough, 1989; Figure 10A, C, E) and primitive-mantle-normalized multi-element plots (Sun and McDonough, 1989; Figure 10B, D, F). Samples of both the Eastern and Western sequence basaltic suites are similar, defining tightly grouped patterns (Figure 10A, B). The Eastern sequence basaltic rocks appear to be less variable in composition than those of the Western sequence (Figure 10A, B). Eastern sequence basalts have mutually parallel multi-element profiles with prominent negative Nb anomalies, and variable, but minor to negligible negative P, Zr–Hf and Ti anomalies. The rocks are moderately light-REE-enriched ($[La/Yb]_{CN}$ = 3.68-4.99) and have a minor negative slope from the middle to the heavy REE ($[Gd/Yb]_{CN}$ = 1.58-1.95). They have minor negative and positive Eu anomalies ([Eu/Eu*] = 0.86-1.21, mean = 1.01). Western sequence basaltic rocks have more variable REE and multi-element patterns, showing similarly prominent negative Nb anomalies, but more pronounced negative P, Zr–Hf and Ti anomalies (Figure 10A, B).

The REE and multi-element patterns of the felsic volcanic rocks show significant greater variability in their incompatible trace-element abundances (Figure 10C, D). Eastern sequence felsic rocks are more variable than those of the Western sequence and exhibit particularly large

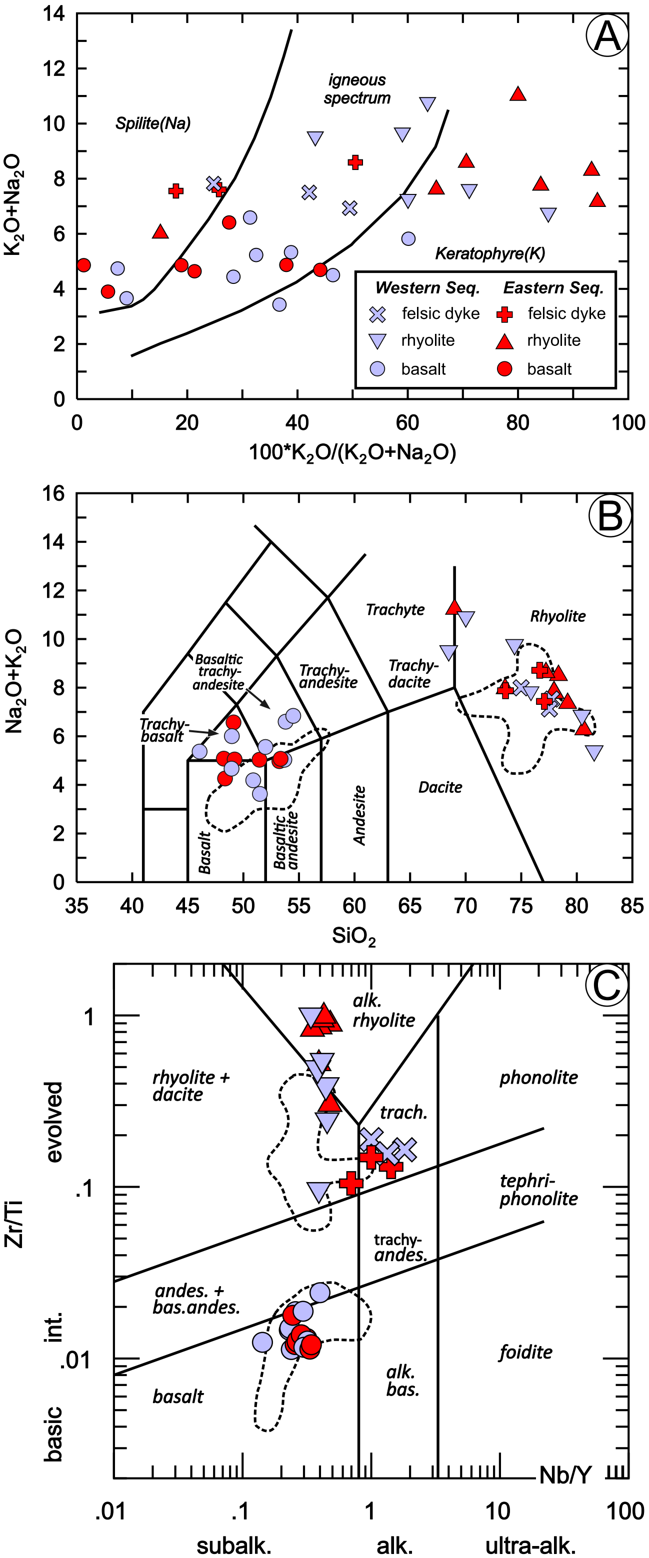

Figure 6. *A) Igneous spectrum plot of Hughes (1973). Samples plotting to the left and right of the central 'igneous spectrum' are likely compositionally altered. B) TAS diagram (LeBas* et al.*, 1986). C) Zr/TiO$_2$ vs Nb/Y discrimination diagram after Pearce (1996) showing the compositions of the Sops Arm rocks. Shown for comparison are fields for selected basalts and rhyolites of the Springdale Group (Coyle, 1990)*

ranges in their LREE, Eu, Sr and TiO_2 abundances. Eastern sequence felsic volcanic rocks have very variable REE abundances ($[La/Yb]_{CN}$ = 0.34–18.1; $[Gd/Yb]_{CN}$ = 0.45–1.69) and prominent but variable negative europium anomalies ([Eu/Eu*] = = 0.18–0.26). Western sequence felsic volcanic rocks form a tight group of mutually parallel REE and multi-element profiles with prominent negative Nb, P, and Ti anomalies, variable negative Eu anomalies ([Eu/Eu*] = = 0.07–0.19) and, an absence of Zr–Hf anomalies. They are light-REE-enriched ($[La/Yb]_{CN}$ = 2.12–16.93) with generally flat heavy-REE segments ($[Gd/Yb]_{CN}$ = 0.84–1.24).

The felsic dykes of both sequences are distinct from the felsic volcanic rocks in having significantly lower abundances of the incompatible trace elements (Figure 10E, F). Three felsic dykes that cut the Jackson's Arm and Frenchmans Cove formations of the Western sequence are variably light-REE-enriched ($[La/Yb]_{CN}$ = 6.10–54.4) with low abundances of the heavy REE (relative to the felsic volcanic rocks) and modest negative Eu anomalies ([Eu/Eu*] = = 0.53–0.81). They exhibit prominent negative P and Ti troughs, very minor negative Zr–Hf anomalies and although exhibit elevated Th, they have highly variable La/Nb ratios (Figure 10E, F). The felsic dykes that cut the Eastern sequence have REE and multi-element profiles similar to those cutting the Western sequence with variably light-REE-enrichment ($[La/Yb]_{CN}$ = 8.18–29.76), low abundances of the heavy REE relative to the felsic volcanic rocks, and have modest Eu anomalies ([Eu/Eu*] = = 0.70–0.88; Figure 10F).

DISCUSSION

New field, petrographic, U–Pb and $^{40}Ar–^{39}Ar$ geochronological data, along with lithogeochemical data for felsic and mafic volcanic rocks and felsic dykes, provide new information on the Sops Arm group and spatially associated rocks, and new constraints on the Silurian to Devonian geodynamic evolution of the region. Field observations indicate that the volcanogenic packages of both the Western and Eastern sequences contain intercalated felsic volcanic, mafic volcanic and conglomeratic rocks that were deposited in dominantly subaerial environments in tectonically active settings. The volcanic products were likely erupted from areally spaced, topographically high, felsic volcanic centres, around which the lavas and their accompanying coarse clastic volcanogenic debris were deposited. Environments more distal from the volcanic centres received finer grained volcanogenic detritus. In such a setting, abrupt lithofacies variations along strike and across strike would be expected, and some of the contrasts in geology from north to south in the group may be related to these effects. For example, the conglomeratic rocks in the northern part of the western

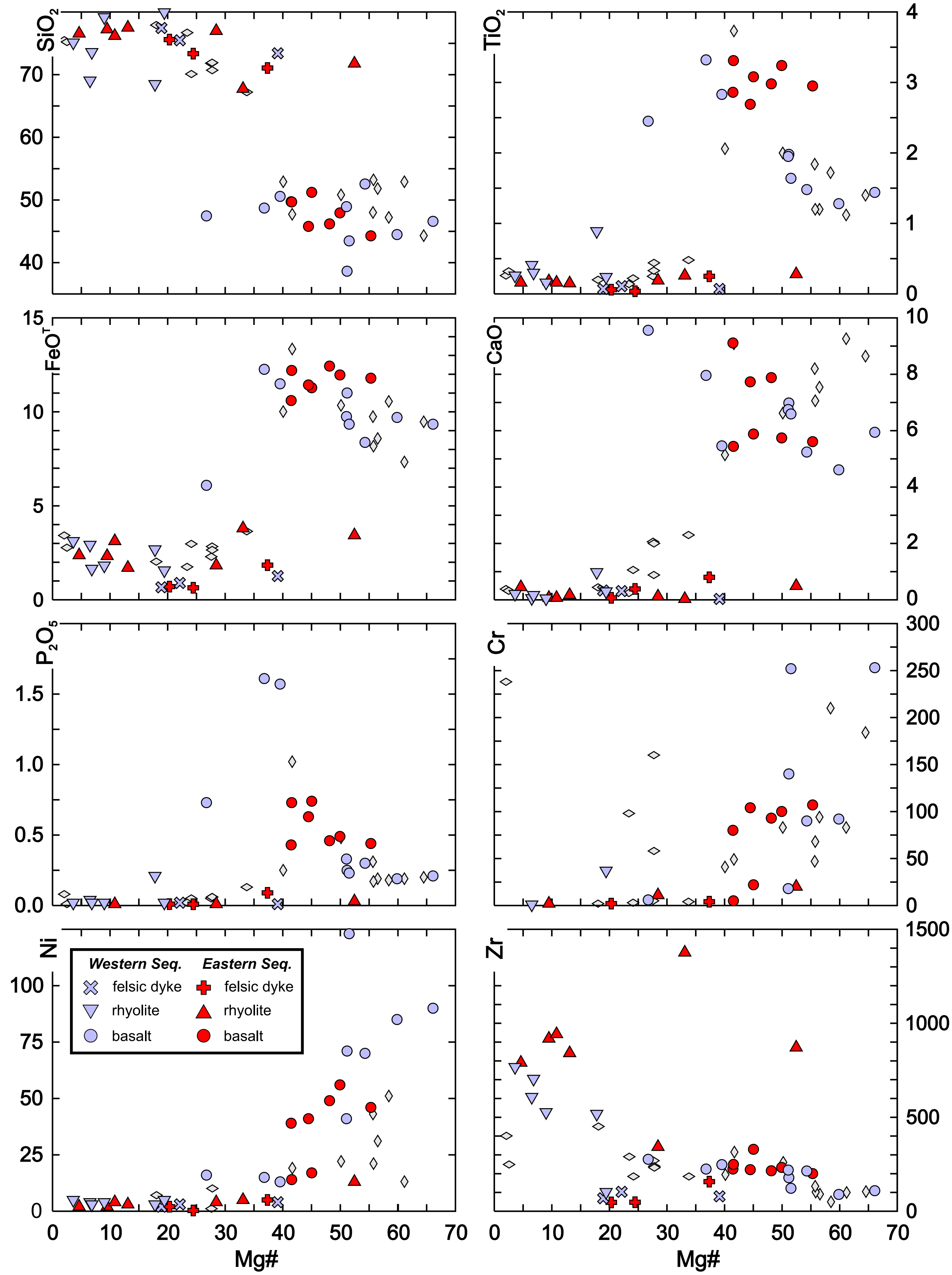

Figure 7. *Selected major and trace elements* vs *Mg# for rocks of the Sops Arm group. Selected analyses of both felsic and mafic volcanic samples of the Silurian Springdale Group (Coyle, 1990: grey diamonds) are shown for comparison.*

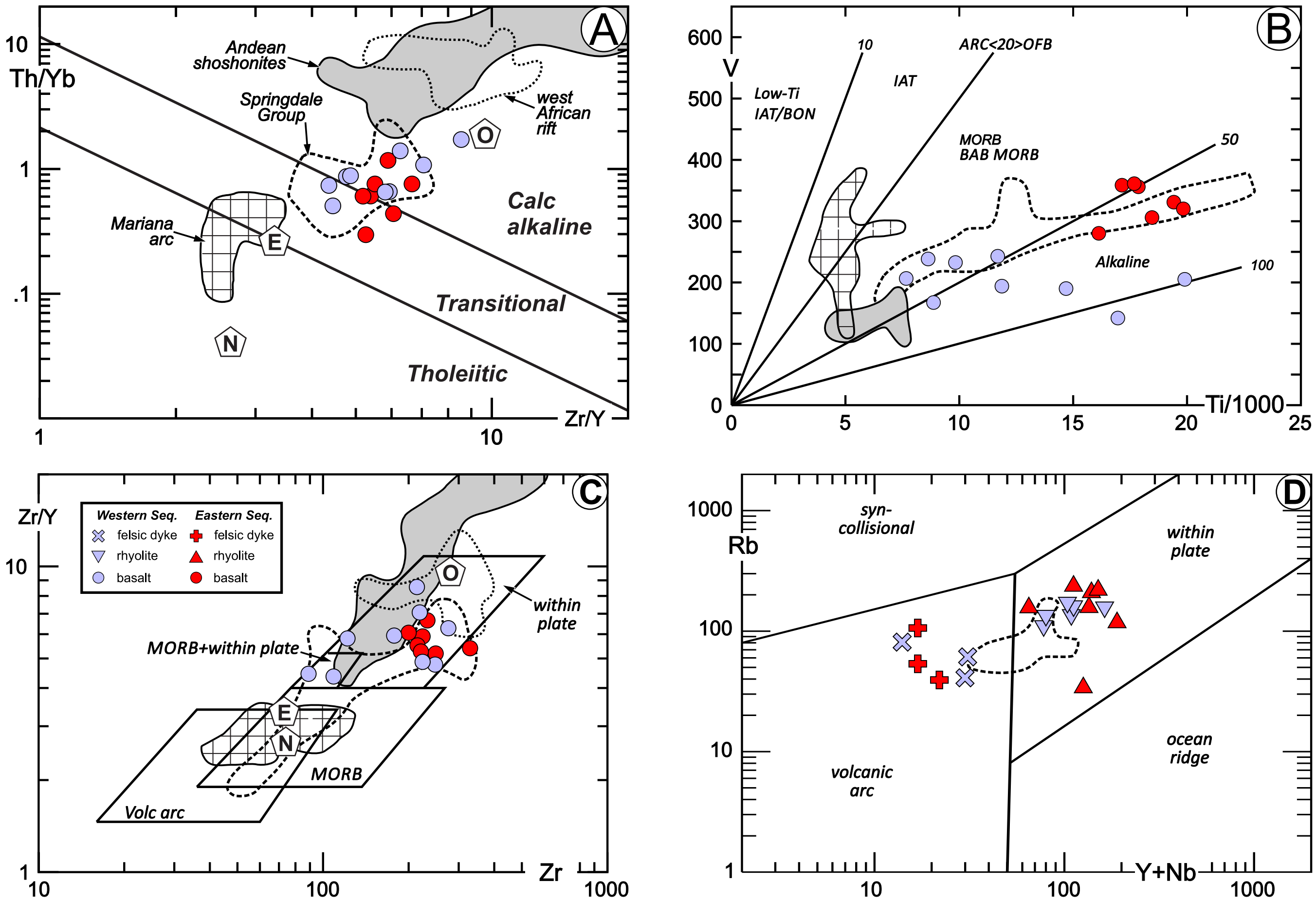

Figure 8. *Major- and trace-element paleotectonic discrimination diagrams. A) Th/Yb* vs *Zr/Y plot of Ross and Bedard (2009). B) V* vs *TiO_2/1000 diagram (Shervais, 1982). C) Zr/Y* vs *Zr diagram (Pearce and Norry, 1979). D) Rb* vs *Y+Nb diagram for felsic rocks (Pearce* et al.*, 1984). Filled grey field represents 38 Oligocene, calc-alkaline to shoshonitic basalts of the central Andes (Sandeman, 1995), cross-hatched field represents basaltic rocks of the Mariana Arc (Elliot* et al.*, 1997) and the dashed field is that for strongly alkaline, rift volcanic rocks of the West Africa Rift (Chakrabati* et al.*, 2009). Key: N = N-MORB; E = E-MORB; O = ocean-island basalt (Sun and McDonough, 1989).*

sequence may be facies equivalents of similar but thinner units in the Pollards Point formation. Intermediate rocks are rare or absent and basalts are more common than previously noted. Rhyolitic to trachytic silicic dykes cut many formations, but are particularly noteworthy in the Jackson's Arm, Frenchmans Cove, Simms Ridge, and Natlins Cove formations. In the upper stratigraphy of the Eastern sequence, these dykes clearly cut bedding in the host rocks, but preserve a weak fabric broadly parallel to the regional structural trends. In the Simms Ridge Formation and the units of the Western sequence, however, the silicic dykes are typically transposed parallel to the local cleavage and/or bedding, thereby obscuring crosscutting relationships. It is not clear therefore if all of the dykes are the same age and that those in the lower parts of the Sops Arm group have simply been more strongly transposed than those cutting the upper parts of the group. The basaltic rocks of both the Western and Eastern sequences, separated by the Long Steady fault, are similar in bulk composition and are transitional to calc-alkaline, continental basalts whose parental magmas were derived at moderate mantle depths, from an enriched, EMORB-like source. These magmas underwent assimilation–fractional crystallization in the middle to upper crust prior to eruption. Felsic volcanic rocks of both the Western and Eastern sequences are evolved, alkaline to peralkaline, within plate-type felsic rocks that have undergone significant feldspar and accessory phase (zircon, allanite) fractionation in the upper crust. Felsic dykes that cut both the Western and Eastern sequences are all similar in composition, are trachytic and have notably lower concentrations of the more compatible trace elements (Nb to Lu; Figure 10) than the felsic volcanic rocks. These appear to represent partial melts of a lower crustal, amphibole ± garnet-bearing intermediate source such as that which may melt to produce Archean tonalite–trondhjemite–granite suites (Figure 9C).

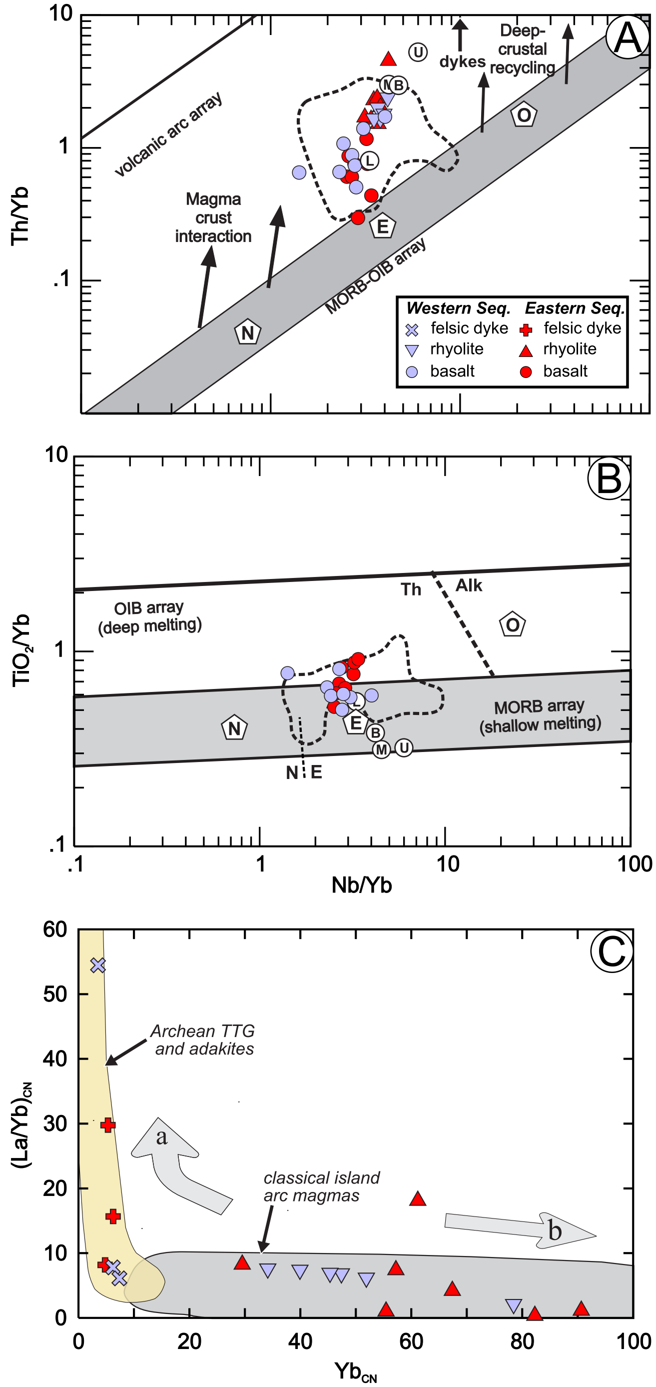

Figure 9. *A) Th/Yb* vs *Nb/Yb and B) TiO_2/Yb* vs *Nb/Yb (after Pearce, 2008) for basaltic rocks of the Sops Arm group. Key: N = N-MORB; E = E-MORB; O = ocean-island basalt (Sun and McDonough, 1989), U – upper cust; M – middle crust; L – lower crust; B – bulk crust (Rudnick and Gao, 2003). Fields as in Figure 8. C) Chondrite-normalized $(La/Yb)_{CN}$* vs *Yb_{CN} (Sun and McDonough, 1989) plot for the felsic rocks. Grey field is for classic island-arc magmas that evolve* via *fractional crystallization whereas the pale yellow field outlines Archean tonalite–trondhjemite–granite suites formed through melting of garnet-bearing crust (adapted from Drummond and Defant, 1990). Grey arrows indicate generalized liquid compositional trends produced during: a) fractional crystallization of hornblende and plagioclase from a tonalitic liquid and; b) fractional crystallization of biotite+plagioclase+potassium feldspar from an intermediate liquid.*

The 434.3 ± 1.1 Ma CA-TIMS U–Pb zircon age for a basal rhyolite (HS13-178A) of the Pollards Point formation of the Western sequence represents one of the oldest Silurian volcanic rocks yet dated in Newfoundland. This Telychian age supports the proposal of van Staal *et al.* (2014), who noted that the Silurian cover sequences in the Newfoundland Appalachians progressively young toward the east, a feature they suggest resulted from a progressive, eastward rollback of the downgoing Ganderian margin and concomitant eastward migration of magmatism and continental redbed sedimentation. The rhyolite dyke (HS13-105B) crystallized at 401.1 ± 0.8 Ma. Although it is broadly concordant with the well-developed regional cleavage, it truncates bedding at a low angle and itself exhibits an internal sericite foliation. The rhyolite was likely intruded relatively late in the regional deformation of the Sops Arm group, or alternatively, the entire package was further tightened during subsequent deformation.

The 401.1 ± 0.8 Ma felsic dyke (HS13-105B) cutting the Simms Ridge formation contains euhedral, undeformed ankerite porphyroblasts, similar to those characterizing much of the lower sections of the Simms Ridge formation near the Long Steady fault (Plate 2B). Therefore it is probable that the precious-metal mineralization at the Browning Mine is younger than the crystallization age of the dyke. The base- and precious-metal-bearing quartz–ankerite veins at the Browning Mine cut a muscovite fabric and are not themselves ductily deformed. Therefore, the 374.2 ± 0.8 Ma ^{40}Ar–^{39}Ar age determination on fabric-forming muscovite from a muscovite–quartz–albite–ankerite schist at the Mine indicates that the final phase of ductile deformation, at temperatures in the range of ~250 to 300°C, is constrained to the interval 401–374 Ma. Precious-metal mineralization occurred at ≤ 374 Ma. Future investigations will include: additional U–Pb geochronology to constrain the age of the Eastern sequence; $^{40}Ar/^{39}Ar$ geochronology on alteration associated with other precious-metal mineralization and; fill-in lithogeochemistry along with Nd isotopic analyses of critical volcanic and epizonal intrusive rocks of the area.

ACKNOWLEDGMENTS

Andy Kerr is warmly thanked for his contribution of figures and suggestions. Matt Minnett, Jonathan Hull, Kendra Power and Chris Voisey provided capable assistance in the field whereas Gerry Hickey helped immensely with logistics and safety. Amanda Langille for excellent work in the U–Pb laboratory at Memorial University. Neil Stapleton and Joanne Rooney of the Geological Survey Branch greatly assisted with figure, map preparation and typesetting. The manuscript was improved by the helpful reviews of Andy Kerr and John Hinchey.

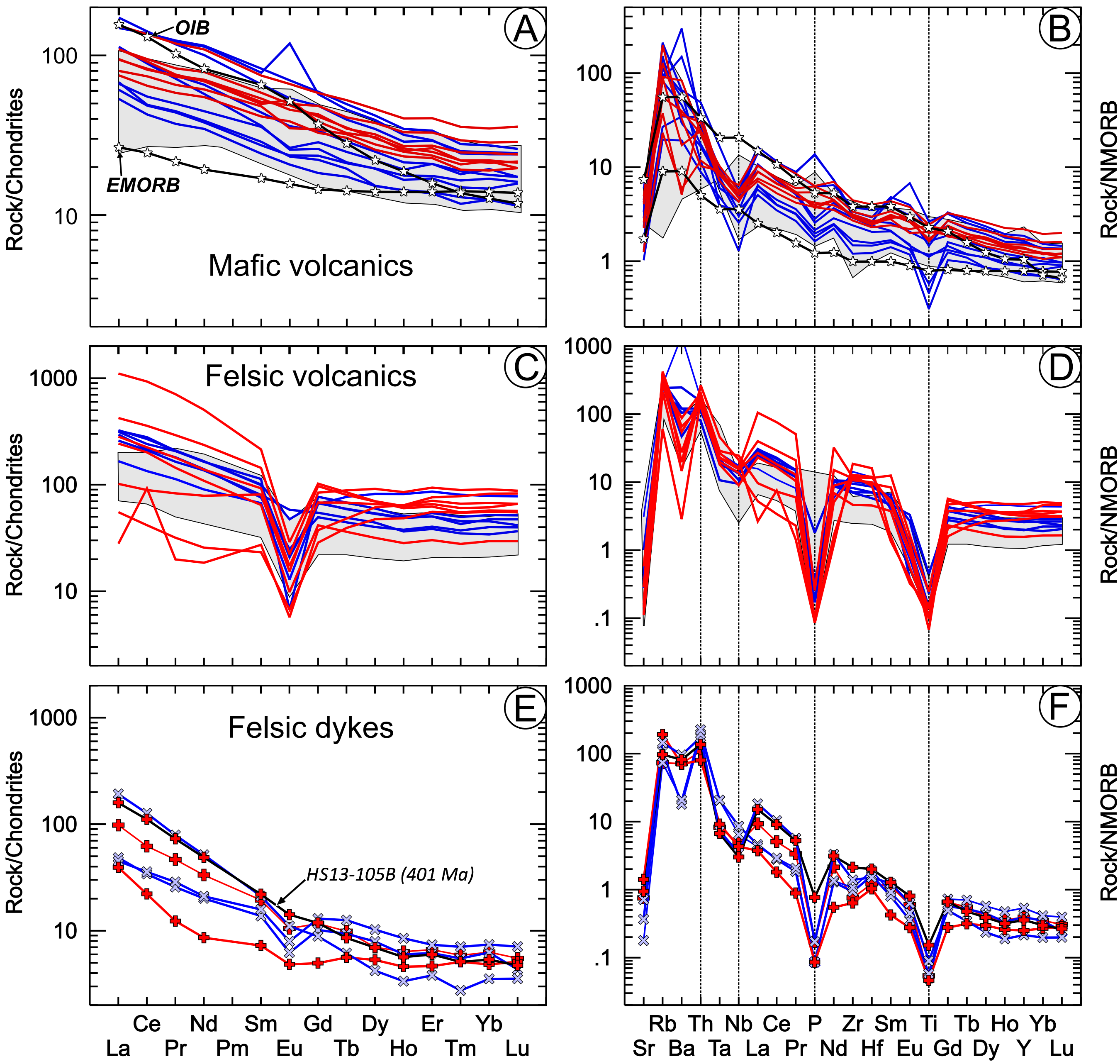

Figure 10. *Chondrite-normalized rare-earth element and primitive-mantle-normalized multi-element plots (Sun and McDonough, 1989) for rocks of the Sops Arm group. A, B) mafic volcanic rocks of the Western and Eastern volcanic sequences compared to the patterns for average EMORB – enriched mid-ocean ridge basalt and OIB – ocean-island basalt (Sun and McDonough, 1989). Also shown is a grey shaded field for nine basaltic rocks of the Springdale Group (Coyle, 1990); C, D) felsic volcanic rocks of the Western and Eastern sequences. A field for nine felsic rocks of the Springdale Group (Coyle, 1990) is shown for comparison; E,F) felsic dyke rocks of the Western and Eastern sequences. Western sequence rocks are represented by blue whereas Eastern sequence rocks are red lines.*

REFERENCES

Berry, W.B.N. and Boucot, A.J.
1970: Correlation of the North American Silurian rocks. Geological Society of America, Special Paper 102, 289 pages.

Betz, F.J.
1948: Geology and mineral deposits of southern White Bay. Newfoundland Geological Survey Bulletin 24, 26 pages.

Boyce, W.D., Ash, J.S. and Dickson, W.L.
1993: The significance of a new bivalve fauna from the Gander map area (NTS 20/15) and a review of Silurian bivalve-bearing faunas in central Newfoundland. *In* Current Research. Government of Newfoundland and Labrador, Department of Mines and Energy, Geological Survey Branch, Report 93-1, pages 187-194.

Chakrabarti, R., Basu, A.R., Santo, A.P., Tedesco, D. and Vaselli, O.
2009: Isotopic and geochemical evidence for a heterogeneous mantle plume origin of the Virunga volcanics, Western rift, East African Rift system. Chemical Geology, Volume 259, pages 273-289.

Churchill, R. and Voordouw, R.
2006: First, second, third, and forth year assessment report documenting reconnaissance prospecting and compilation for map staked licenses 09287M (Wizard Property) and 08878M, 10935M, and 12734M (Viking Property), White Bay Area, Newfoundland, NTS sheets 12H/10 and 12H/11. Assessment report for Altius Resources, 137 pages, 7 figures, 3 maps.

Colman-Sadd, S., Hayes, J.P. and Knight, I.
1990: Geology of the Island of Newfoundland. Government of Newfoundland and Labrador, Department of Mines and Energy, Geological Survey Branch, Map 90-01.

Coyle, M.
1990: Geology, geochemistry and geochronology of the Springdale Group, an Early Silurian Caldera in central Newfoundland. Unpublished Ph.D. thesis, Memorial University of Newfoundland, St John's, Newfoundland, Canada, 381 pages.

Dalrymple, G.B., Alexander, Jr., E.C., Lanphere, M.A. and Kraker, G.P.
1981: Irradiation of samples for $^{40}Ar/^{39}Ar$ dating using the Geological Survey TRIGA Reactor. U.S. Geological Survey, Professional Paper 1176, 55 pages.

Drummond, M.S. and Defant, M.J.
1990: A model for trondhjemite-tonalite-dacite genesis and crustal growth via slab melting: Archean to modern comparisons. Journal of Geophysical Research, Volume 95, pages 21503-21521.

Dunning, G.R.
1987: U/Pb geochronology of the Coney Head Complex, Newfoundland. Canadian Journal of Earth Sciences, Volume 24, pages 1072-1075.

Ebert, S
2008: Sixth year assessment report on geological, geochemical and trenching exploration for licence 14079M on claims in the White Bottom Pond area, White Bay, Newfoundland. Altius Resources Incorporated and Northern Abitibi Mining Corporation. Newfoundland and Labrador Geological Survey, Assessment File 12H/1876, 67 pages.

2009: Seventh year assessment report on geological, geochemical, trenching and diamond drilling exploration for licence 14079M on claims in the White Bottom Pond area, White Bay, Newfoundland. Northern Abitibi Mining Corporation and Altius Resources Incorporated. Newfoundland and Labrador Geological Survey, Assessment File 12H/2003, 237 pages.

2010: Eighth year assessment report on remote sensing and geological, geochemical, trenching and diamond drilling exploration for licence 14079M on claims in the White Bottom Pond area, White Bay, Newfoundland. Northern Abitibi Mining Corporation. Newfoundland and Labrador Geological Survey, Assessment File 12H/2155, 853 pages.

Elliott, T., Plank, T., Zindler, A., White, W. and Bourdon, B.
1997: Element transport from slab to volcanic front at the Mariana arc. Journal of Geophysical Research, Volume 102, pages 14991-15019.

Erdmer, P.
1986: Geology of the Long Range Inlier in the Sandy Lake map area, western Newfoundland. *In* Current Research, Part B. Geological Survey of Canada, Paper 86-1B, pages 19-27.

Fitzpatrick, D. and Osmond, R.T.
2010: First year assessment report on prospecting and geochemical and geophysical exploration for licences 15650M-15654M and 16396M on claims in the Main River area, White Bay, western Newfoundland, 2 reports. 1289839 Alberta Limited. Newfoundland and Labrador Geological Survey, Assessment File 12H/2036, 126 pages.

Froude, T.
2011a: Third and fourth year assessment report on prospecting and geochemical, trenching and diamond drilling exploration for licences 12713M and 17095M-17096M on claims in the White Bottom Pond area, White Bay, western Newfoundland. Spruce Ridge Resources Limited. Newfoundland and Labrador Geological Survey, Assessment File 12H/2150, 255 pages.

2011b: Fourth year year assessment report on compilation and airborne reconnaissance for licence 17095M on claims in the Doucers Valley area, White Bay, Newfoundland. Spruce Ridge Resources Limited. Newfoundland and Labrador Geological Survey, Assessment File 12H/2114, 21 pages.

Harris, J.
2008: Eighth year assessment report on geophysical and diamond drilling exploration and licences 13768M on claims in the Jackson's Arm area, White Bay, Newfoundland. Kermode Resources Limited, South Coast Ventures Incorporated and Cornerstone Resources. Newfoundland and Labrador Geological Survey, Assessment File 12H/15/1987, 329 pages.

Heaman, L.M., Erdmer, P. and Owen, J.V.
2002: U-Pb geochronologic constraints on the crustal evolution of the Long Range Inlier, Newfoundland. Canadian Journal of Earth Sciences, Volume 39, pages 845-860.

Hendriks, M., Jamieson, R.A., Zentilli, M. and Reynolds, P.H.
1992: Exhumation of crystalline basement rocks: low-temperature thermochronology of the Long Range Inlier. *In* Low-temperature Thermochronology. *Edited by* M. Zentilli and P.H. Reynolds. Mineralogical Association of Canada, Short Course Handbook 20, pages 119-139.

Heyl, G.R.
1937: The geology of the Sop's Arm area, White Bay, Newfoundland. Newfoundland Department of Natural Resources, Geology Section, Bulletin 8, 42 pages.

Hughes, C.J.
1973: Spilites, keratophyres, and the igneous spectrum. Geological Magazine, Volume 109, pages 513-527.

Kamo, S. and Gower, C.F.
1994: U-Pb baddeleyite dating clarifies age of characteristic paleomagnetic remanence of Long Range dykes, southeastern Labrador. Atlantic Geology, Volume 30, pages 259-262.

Kamo, S., Gower, C.F. and Krogh, T.E.
1989: A birthdate for the Iapetus ocean? A precise U-Pb zircon and baddeleyite age for the Long Range dykes, S.E. Labrador. Geology, Volume 17, pages 602-605.

Kerr, A.
2003: Cambro-Ordovician sedimentary rocks of western White Bay: stratigraphy, structure and potential for carlin-type gold mineralization. *In* Report of Activities. Government of Newfoundland and Labrador, Department of Mines and Energy, Geological Survey, Report of Activities, pages 8-12.

2004: An overview of sedimentary-rock-hosted gold mineralization in western White Bay (NTS map area 12H/15). *In* Current Research. Government of Newfoundland and Labrador, Department of Mines and Energy, Geological Survey, Report 04-1, pages 23-42.

2006a: Silurian rocks of the Sops Arm group, western Newfoundland: some new food for future digestion. *In* Current Research. Government of Newfoundland and Labrador, Department of Natural Resources, Geological Survey, Report 06-1, pages 91-117.

2006b: Mesothermal gold mineralization in the Silurian Sops Arm group, western Newfoundland: a descriptive and historical overview. *In* Current Research. Government of Newfoundland and Labrador, Department of Natural Resources, Geological Survey, Report 06-1, pages 61-90.

Kerr, A. and Knight, I.
2004: Preliminary report on the stratigraphy and structure of Cambrian and Ordovician rocks in the Coney Arm area, western White Bay (NTS map area 12H/15). *In* Current Research. Government of Newfoundland and Labrador, Department of Mines and Energy, Geological Survey, Report 04-1, pages 127-156.

Kerr, A. and van Breemen, O.
2007: The timing of gold mineralization in White Bay, western Newfoundland: Evidence from ^{40}Ar–^{39}Ar studies of mafic dykes that predate and postdate mineralization. Atlantic Geology, Volume 43, pages 148-162.

Le Bas, M.J., Le Maitre, R.W., Streckeisen, A. and Zanettin, B.
1986: A chemical classification of volcanic rocks based on the total alkali silica diagram. Journal of Petrology, Volume 27, Number 3, pages 745-750.

Lock, B.E.
1969a: The Lower Paleozoic geology of western White Bay, Newfoundland. Unpublished Ph.D. thesis, Cambridge University, Cambridge, England, 343 pages.

1969b: Silurian rocks of west White Bay area, Newfoundland. *In* North Atlantic - Geology and Continental Drift. *Edited by* M.M. Kay. American Association of Petroleum Geologists, Memoir 13, pages 433-442.

Ludwig, K.R.
2008: User's Manual for ISOPLOT 3.60 - A Geochronological Toolkit for Microsoft Excel. Berkeley Geochronological Centre Special Publication Number 4, 54 pages.

Martin, W.
1983: Once Upon a Mine: Story of pre-Confederation Mines on the Island of Newfoundland. Canadian Institute of Mining and Metallurgy, Special Volume 26, 98 pages.

Mattinson, J.M.
2005: Zircon U–Pb chemical abrasion (CA-TIMS) method; combined annealing and multi-step partial dissolution analysis for improved precision and accuracy of zircon ages. Chemical Geology, Volume 220, pages 47-66.

McDougall, I. and Harrison, T.M.
1988: Geochronology and Thermochronology by the ^{40}Ar-^{39}Ar Method: Oxford Monographs on Geology and Geophysics #9, Oxford, United Kingdom, Oxford University Press, 212 pages.

McLennon, T.
2010: Third year assessment report on prospecting and geochemical exploration for licence 13301M on claims in the Natlins Brook area, White Bay, Newfoundland. Newfoundland and Labrador Geological Survey, Assessment File 12H/10/2050, 23 pages.

Minnett, M.
2012: An investigation of the geology, geochemistry, and timing of gold mineralization at the Viking Gold Deposit, White Bay, Newfoundland. Unpublished M.Sc. thesis, Memorial University of Newfoundland, St. John's, Canada, 139 pages.

Minnett, M., Sandeman, H. and Wilton, D.
2010: Regional setting of gold mineralization at the Viking Property, southern White Bay, Newfoundland. *In* Current Research. Government of Newfoundland and Labrador, Department of Natural Resources, Geological Survey, Report 10-1, pages 51-64.

2012: Geochemistry of the host rocks and timing of gold-electrum mineralization at the Viking Property, Newfoundland. *In* Current Research. Government of Newfoundland and Labrador, Department of Natural Resources, Geological Survey, Report 12-1, 61-84.

Murphy, N.G. and Smith, G.
2007: Second year assessment report on compilation and geophysical exploration for licences 11143M and 11145M on claims in the Sops Arm area, White Bay, Newfoundland, 2 reports. Newfoundland and Labrador Geological Survey, Assessment File 12H/10/1877, 44 pages.

Neale, E.R.W. and Nash, W.A.
1963: Sandy Lake (east half), Newfoundland. Geological Survey of Canada, Paper 62-28, 40 pages.

O'Driscoll, J., Patey, B. and Churchill, R.
2011: Second year assessment report on geological and geochemical exploration for licences 17547M and 17549M-17550M on claims in the Doucers Valley area, White Bay, Newfoundland. Altius Resources Incorporated. Newfoundland and Labrador Geological Survey, Assessment File 12H/15/2137, 47 pages.

Patey, B.
2010: First year assessment report on prospecting and geochemical exploration for licences 17547M and 17549M-17550M on claims in the Doucers Valley area, White Bay, Newfoundland. Altius Resources Incorporated. Newfoundland and Labrador Geological Survey, Assessment File 12H/15/2105, 71 pages.

Patey, B. and King, L.
2010: First year assessment report on prospecting and geochemical exploration for licences 15657M-15658M on claims in the Jackson's Arm area, White Bay, Newfoundland. Newfoundland and Labrador Geological Survey, Assessment File 12H/15/2097, 56 pages.

Pearce, J.A.
1996: A user's guide to basalt discrimination diagrams. Geological Association of Canada, Short Course Notes, Volume 12, pages 79-113.

2008: Geochemical fingerprinting of oceanic basalts with applications to ophiolite classification and the search for Archean oceanic crust. Lithos, Volume 100, pages 14-48.

Pearce, J.A., Harris, N.B.W. and Tindle, A.G.
1984: Trace element discrimination diagrams for the tectonic interpretation of granitic rocks. Journal of Petrology, Volume 25, pages 956-983.

Pearce, J.A. and Norry, M.J.
1979: Petrogenetic implications of Ti, Zr, Y and Nb variations in volcanic rocks. Contributions to Mineralogy and Petrology, Volume 69, pages 33-47.

Reid, W.
2009: Second year and sixth year supplementary assessment report on prospecting and geochemical exploration for licences 9074M, 12906M, 12908M, 12994M-12995M, 13007M-13008M, 13034M, 13052M, 13077M and 15720M-15731M on claims in the Sops Arm and Sheffield Lake area, western Newfoundland. Metals Creek Resources Limited. Newfoundland and Labrador Geological Survey, Assessment File 12H/1951, 84 pages.

Reid, W., Greenwood, R. and Largeaud, J.
2008: First, second and sixth year assessment report on geophysical exploration for licences 9074M, 12902M-12908M, 12994M-12995M, 12999M, 13007M-13008M, 13034M, 13040M, 13052M, 13072M-13078M, 13978M, 14088M, 14289M and 14411M on claims in the Sops Arm, Baie Verte Junction and Sheffield Lake area, western Newfoundland, 2 reports. Metals Creek Resources Limited, Quinlan, E and Quinlan Prospecting. Newfoundland and Labrador Geological Survey, Assessment File 12H/1898, 61 pages.

Reid, W. and Myllyaho, J.
2012: First year assessment report on prospecting, geochemical and trenching exploration for licences 18403M, 19525M, 19530M and 19542M on claims in the Jacksons Arm area, White Bay, Newfoundland. Newfoundland and Labrador Geological Survey, Assessment File 12H/15/2066, 2012, 84 pages.

Reynolds, P.H.
1992: Low temperature thermochronology by the ^{40}Ar-^{39}Ar method. *In* Low Temperature Thermochronology. *Edited by* M. Zentilli and P.H. Reynolds. Mineralogical Association of Canada, pages 3-19.

Ross P. and Bedard, J.H.
2009: Magmatic affinity of modern and ancient subalkaline volcanic rocks determined from trace-element discrimination diagrams. Canadian Journal of Earth Sciences, Volume 46, pages 823-839.

Rudnick, R.L. and Gao, S.
2003: Composition of the continental crust. Treatise on Geochemistry, Volume 3, pages 1-64.

Sandeman, H.A.I.
1995: Lithostratigraphy, petrology and geochronology of the Crucero Supergroup, Puno, SE Peru: Implications for the Cenozoic geodynamic evolution of the Southern Peruvian Andes. Unpublished Ph.D. thesis, Queen's University, Kingston, 381 pages.

Sandeman, H.A.I. and McNicoll, V.J.
2015: Age and petrochemistry of rocks from the Aucoin gold prospect (NTS map area 13N/6) Hopedale block, Labrador: Late Archean, alkali monzodiorite-syenite hosts Proterozoic orogenic Au–Ag–Te mineralization. *In* Current Research. Government of Newfoundland and Labrador, Department of Natural Resources, Geological Survey, Report 15-1, pages 85-103.

Saunders, C.M. and Smyth, W.R.
1990: Geochemical characteristics of the Gull Lake intrusive suite and Devils Room Granite, western White Bay, Newfoundland. *In* Current Research. Newfoundland Department of Mines and Energy, Geological Survey Branch, Report 90-1, pages 183-199.

Shervais, J.W.
1982: Ti-V plots and the petrogenesis of modern ophiolitic lavas. Earth and Planetary Science Letters, Volume 59, pages 101-118.

Shrock, R.R. and Twenhofel, W.H.
1939: Silurian fossils from northern Newfoundland. Journal of Paleontology, Volume 13, pages 241-266.

Smyth, W.R. and Schillereff, H.S.
1982: The Pre-Carboniferous geology of southwest White Bay. *In* Current Research. Government of Newfoundland and Labrador, Department of Mines and Energy, Mineral Development Division, Report 82-1, pages 78-98.

Sparkes, G.W. and Dunning, G.R.
2014: Late Neoproterozoic epithermal alteration and mineralization in the western Avalon Zone: a summary of mineralogical investigations and new U/Pb geochronological results. *In* Current Research. Government of Newfoundland and Labrador, Department of Natural Resources, Geological Survey, Report 14-1, pages 99-128.

Stacey, J.S. and Kramers, J.D.
1975: Approximation of terrestrial lead isotope evolution by a two stage model. Earth and Planetary Science Letters, Volume 26, pages 207-221.

Steiger, R.H. and Jäger, E.
1977: Subcommission on geochronology: Convention on the use of decay constants in geo- and cosmochronology. Earth and Planetary Science Letters, Volume 36, pages 359-362.

Sun, S.S. and McDonough, W.F.
1989: Chemical and isotopic systematics of ocean basalts: implications for mantle composition and processes. Geological Society, Special Publication 42, pages 313-345.

Thurlow, J.G., Churchill, R. and Smith, G.
2007: Assessment report on geophysical exploration for 2006 submission for Mining Lease 60 and for second year, second year supplementary, fourth year, fourth year supplementary, fifth year and sixth year supplementary assessment on licences 7897M, 8647M, 8878M, 8913M, 9287M, 10141M, 10727M and 10935M on claims in the Rocky Brook and White Bay areas, western Newfoundland, 2 reports. Altius Resources Incorporated, JNR Resources Incorporated, Spruce Ridge Resources and Bidgood, R. Newfoundland and Labrador Geological Survey, Assessment File 12H/1850, 41 pages.

Tuach, J.
1987: Mineralized environments, metallogenesis, and the Doucers Valley fault complex, western White Bay: a philosophy for gold exploration in Newfoundland. *In* Current Research. Government of Newfoundland and Labrador, Department of Mines and Energy, Mineral Development Division, Report 87-1, pages 129-144.

van Staal, C., Whalen, J.B., Valverde-Vaquero, P., Zagorevski, A. and Rogers, N.
2009: Pre-Carboniferous, episodic accretion-related, orogenesis along the Laurentian margin of the northern Appalachians. Geological Society of London, Special Publication 327, pages 271-316.

van Staal, C., Zagorevski, A., McNicoll, V. and Rogers, N.
2014: Time-transgressive Salinic and Acadian orogenesis, magmatism and Old Red sandstone sedimentation in Newfoundland. Geoscience Canada, Volume 41, pages 138-164.

Williams, H.
1977: The Coney Head Complex: another Taconic allochthon in west Newfoundland. American Journal of Science, Volume 277, pages 1279-1295.